© 2020. Published by The Company of Biologists Ltd | Development (2020) 147, dev185298. doi:10.1242/dev.185298

RESEARCH ARTICLE

Hox13 genes are required for mesoderm formation and axis elongation during early zebrafish development

Zhi Ye and David Kimelman*

ABSTRACT

The early vertebrate embryo extends from anterior to posterior due to the addition of neural and mesodermal cells from a neuromesodermal progenitor (NMp) population located at the most posterior end of the embryo. In order to produce mesoderm throughout this time, the NMps produce their own niche, which is high in Wnt and low in retinoic acid. Using a loss-of-function approach, we demonstrate here that the two most abundant Hox13 genes in zebrafish have a novel role in providing robustness to the NMp niche by working in concert with the niche-establishing factor Brachyury to allow mesoderm formation. Mutants lacking both *hoxa13b* and *hoxd13a* in combination with reduced Brachyury activity have synergistic posterior body defects, in the strongest case producing embryos with severe mesodermal defects that phenocopy *brachyury* null mutants. Our results provide a new way of understanding the essential role of the Hox13 genes in early vertebrate development.

This article has an associated 'The people behind the papers' interview.

KEY WORDS: Hox genes, Brachyury, Wnt signaling, Neuromesodermal progenitors

INTRODUCTION

A hallmark of early embryonic vertebrate development is the progressive formation of the posterior embryonic body from anterior to posterior (Kimelman and Martin, 2012; Steventon and Martinez Arias, 2017). This is clearly seen with the production of somites, which first form just behind the head and are then added sequentially until the final anterior-posterior (A-P) axis of the embryo is established (Holley, 2007; Pourquié, 2018). A key component of this process is a bipotential neuromesodermal cell progenitor (NMp) population located at the most posterior end of the embryo (the tailbud) during the somite-forming stages, which produces both the spinal cord and musculature (Gouti et al., 2015; Henrique et al., 2015; Kimelman, 2016b; Martin, 2016; Steventon and Martinez Arias, 2017; Wilson et al., 2009). The NMps express both the neural gene *sox2* and the mesodermal gene *T/Brachyury* (known as *tbxta* or *no tail* in zebrafish), allowing them to differentiate in either a neural or mesodermal direction. The canonical (β-catenin-dependent) Wnt signaling pathway plays a key role in regulating this switch, such that NMps exposed to high Wnt enter the presomitic mesoderm and differentiate into various mesodermal fates such as muscle, whereas those deprived of Wnt signaling become neural tissue. This mechanism allows the embryo to carefully balance the ratio of spinal cord to somites along the entire A-P axis, although in amniotes it occurs over a prolonged period, whereas in anamniotes the fate decisions largely occur during gastrulation (Martin and Kimelman, 2012; Steventon and Martinez Arias, 2017).

What causes the termination of the embryonic A-P axis is uncertain. The simplest explanation is that the NMps, which progressively differentiate during the somitogenesis stages, are eventually depleted, resulting in completion of the A-P axis. An intriguing alternative idea is that the most 5′ Hox genes (paralog group 13) actively terminate posterior extension along the A-P axis (Aires et al., 2019; Amin et al., 2016; Denans et al., 2015; Mallo, 2018; Steventon and Martinez Arias, 2017; Young et al., 2009). The initial impetus for this view came from the observation that knockout of the mouse *Hoxb13* gene caused the addition of two small somites at the tip of the tail, extending the embryo to 67 somites (Economides et al., 2003). Curiously, knockout of the other Hox13 paralogs in mouse did not cause a lengthening of the body axis (Dolle et al., 1993; Fromental-Ramain et al., 1996; Godwin and Capecchi, 1998; Suemori and Noguchi, 2000).

Additional support for the proposed role of Hox13 genes in terminating the A-P axis in mouse came from experiments in which *Hoxa13*, *Hoxb13* and *Hoxc13* were overexpressed using a strong transcriptional promoter, resulting in embryos lacking all or most of the tail (Aires et al., 2019; Young et al., 2009). Additionally, chick embryos overexpressing *Hoxa13*, *Hoxb13* and *Hoxc13*, but not *Hoxd13*, showed slower ingression of mesodermal cells into the somites from the tailbud (Denans et al., 2015). Moreover, these authors showed that *Hoxa13* overexpression caused a reduction in the levels of the endogenous *T/Brachyury* gene, apparently through downregulation of the Wnt signaling pathway. This led to their proposal that a key job of the Hox13 genes is to reduce the size of the presomitic mesoderm by progressively reducing canonical Wnt signaling.

A major caveat to the proposal that Hox13 genes limit the length of the A-P axis is that, with the one exception of the mouse *Hoxb13* mutant that causes a minor increase in the number of somites (as well as overgrowth of posterior neural tissue causing a wider and longer spinal cord), it is based on overexpression studies. We chose instead to take a loss-of-function approach in zebrafish using CRISPR to mutate the two most abundant Hox13 genes in the tailbud. We show here that loss of *hoxa13b* or a combined loss of *hoxa13b* and *hoxd13a* does not cause posterior defects in an otherwise wild-type background. However, we show that *hoxa13b* and *hoxd13a* genes genetically interact with *tbxta*, the zebrafish ortholog of *T/Brachyury*, such that a combined reduction in Tbxta activity and loss of *hoxa13b* and *hoxd13a* leads to severe synergistic posterior embryonic defects. We show that these defects are due to a

Department of Biochemistry, University of Washington, Seattle, WA 98195-7350, USA.

*Author for correspondence (kimelman@uw.edu)

D.K., 0000-0002-9261-4506

Handling Editor: James Briscoe
Received 2 October 2019; Accepted 19 October 2020

Development (2020) 147, dev185298. doi:10.1242/dev.185298

loss of mesoderm and a concomitant increase in *sox2*-expressing cells, which parallels a sharp reduction in the expression of the posterior canonical Wnt genes and the retinoic acid (RA)-degrading enzyme Cyp26a1, as is observed in *tbxta* null mutants. Finally, using a newly created zebrafish line that overexpresses Hoxa13b we show that gain of function of Hox13 protein is not the opposite of loss of function, suggesting that Hox13 gene overexpression studies have the potential to be misleading. We propose that the essential role of Hox13 genes is to provide robustness to the Brachyury-dependent NMp niche, which maintains Wnt signaling as well as preventing RA from accumulating in the tailbud, allowing the NMps to differentiate as mesoderm.

RESULTS

hoxa13b mutants are phenotypically normal

Zebrafish have six paralogs of the Hox13 cluster: *hoxa13a*, *hoxa13b*, *hoxb13a*, *hoxc13a*, *hoxc13b* and *hoxd13a*. Using data from a previous RNA sequencing (RNA-seq) analysis of the tailbuds of mid-somitogenesis zebrafish embryos (Kimelman et al., 2017), we observed that all genes except *hoxb13a* are expressed at significant levels in the tailbud. We therefore made *in situ* hybridization probes to all the Hox13 genes except *hoxb13a* and observed that each of these is expressed in the tailbud at mid-somitogenesis, as expected (Fig. 1A). To determine the relative abundance of each of the Hox13 genes we used quantitative PCR, and found that *hoxa13b* and *hoxd13a* were the most abundant and were expressed at similar levels, with the remainder of the Hox13 genes being expressed at lower levels. This result was also observed in tailbud RNA-seq data (Kimelman et al., 2017).

Of the two most abundant Hox13 genes, we initially focused on *hoxa13b* because a previous overexpression study reported that *Hoxa13* inhibited mesodermal cell movements out of the chick tailbud, whereas *Hoxd13* had no effect (Denans et al., 2015). Zebrafish *hoxa13b* is expressed in the future posterior mesoderm as early as the end of gastrulation, and continues to be expressed there until the end of somitogenesis (Fig. 1B). The initial expression of *hoxa13b* at such an early stage of embryogenesis seemed surprising for a gene proposed to be involved in terminating axis formation. Therefore, we generated a mutant allele of *hoxa13b* that removed 16 bp in the middle of the coding region, eliminating the essential DNA binding region (Fig. 2A). Embryos homozygous for $hoxa13b^{\Delta 16}$ were phenotypically completely normal, as were adults obtained from these embryos. One possibility for the lack of phenotype is compensation by the other Hox13 genes triggered by nonsense-mediated decay, as observed in zebrafish for other transcripts with a premature termination codon (Ma et al., 2019). However, using qPCR we observed that $hoxa13b^{\Delta 16}$ was expressed at the same level as wild-type *hoxa13b*, and that the other Hox13 genes were not upregulated in $hoxa13b^{\Delta 16}$ homozygous mutant embryos (not shown).

hoxa13b and *hoxa13b;d13a* mutants show posterior defects at lower temperatures

An alternative possibility for the lack of phenotype in zebrafish $hoxa13b^{\Delta 16}$ embryos is that the other Hox13 genes are redundant with *hoxa13b*. We therefore mutated the other abundant Hox13 gene, *hoxd13a*, starting with adults that were homozygous for the $hoxa13b^{\Delta 16}$ mutation. Analysis of *hoxd13a* expression revealed that it is also activated early during somitogenesis, starting at the eight-somite stage (Fig. S1). We obtained three *hoxd13a* mutations, which inserted either 4 or 13 base pairs in the middle of the *hoxd13a* coding region, or deleted 8 base pairs at this site, with all of the mutations eliminating the DNA binding domain (Fig. 2A). In crosses of heterozygous adults we observed embryos with low levels of tail defects from mild to severe (crosses of $hoxa13b^{\Delta 16/\Delta 16}$; $hoxd13a^{ins13/+}$ fish produced 4.2% defective embryos, n=188; Fig. 2B), with a very small number of these defective embryos surviving to adulthood (Fig. S2). We observed a strong selection bias against double mutant females, but were able to obtain one double mutant female ($hoxa13b^{\Delta 16/\Delta 16}$;$hoxd13a^{ins4/ins4}$). Crossing this to a double mutant male of the same genotype produced 12.5% defective embryos (n=40). These results demonstrate that *hoxa13b*

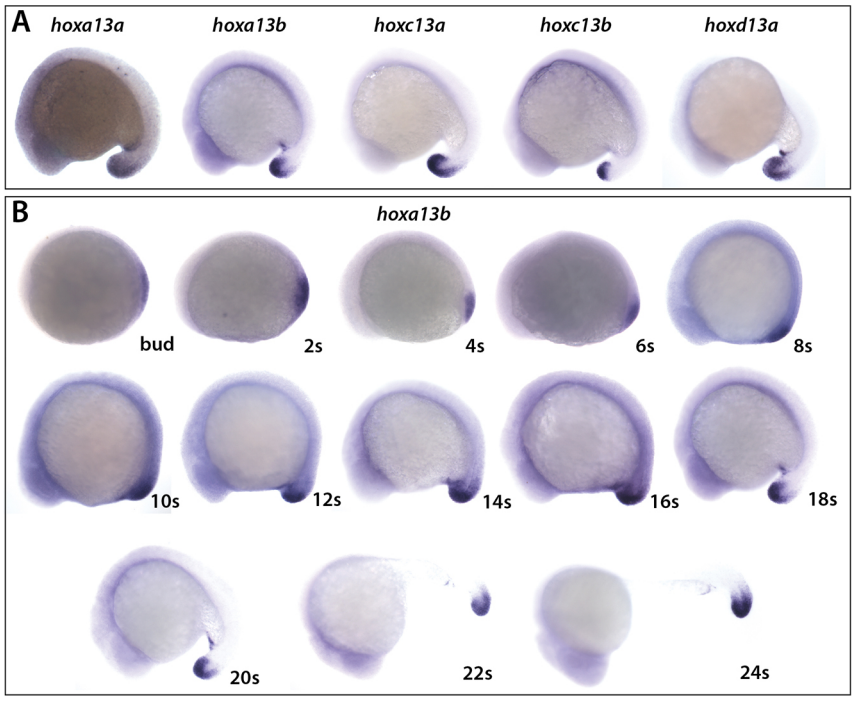

Fig. 1. *hoxa13b* is expressed from early stages. (A) Expression of the five posteriorly expressed Hox13 genes at the 18-somite stage. The embryos were allowed to develop for different lengths of time to optimally show expression of each of the genes and do not reflect the relative levels of expression. (B) Expression of *hoxa13b* from the end of gastrulation (bud stage) until the 24-somite stage (24 s). Embryos from 8 s to 24 s were developed for the same length of time. Embryos from bud to 6 s were developed 50% longer.

Development (2020) 147, dev185298. doi:10.1242/dev.185298

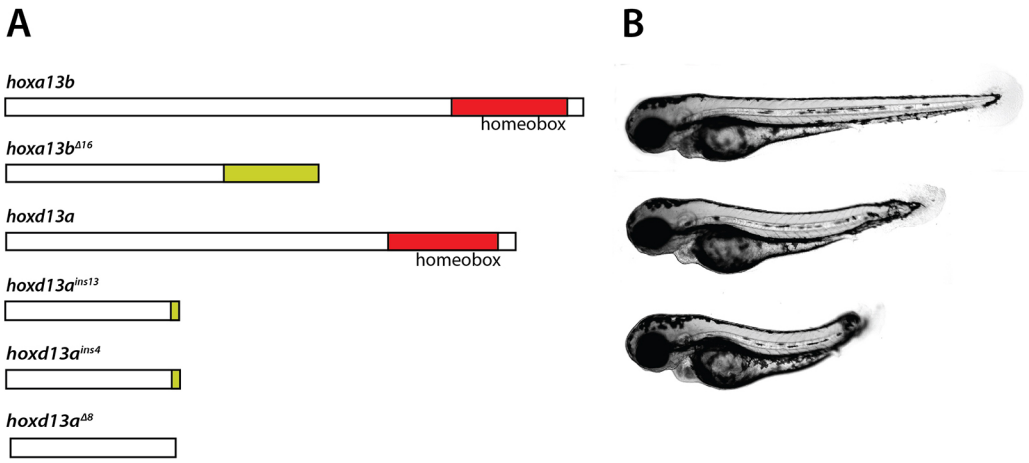

Fig. 2. *hoxa13;d13* mutants have posterior defects. (A) Scheme of Hox13 mutants. The coding regions of *hoxa13b* and *hoxd13a* are shown, with the DNA binding homeobox indicated. The *hoxa13b*$^{\Delta 16}$ mutant is truncated due to a 16 base pair (bp) deletion that causes a frameshift, adding additional amino acids (green). Three *hoxd13a* mutants are shown, with insertions of 13 or 4 bp or a deletion of 8 bp. The 8 bp deletion causes an immediate truncation, whereas the insertion mutants cause frameshifts that add a small number of additional amino acids. (B) Posterior defects observed in *hoxa13*$^{\Delta 16}$*;hoxd13a*^{ins13} mutants (lower two embryos) compared with a wild-type embryo (top) at 3 dpf.

and *hoxd13a* are redundant because posterior defects appear when both Hox13 genes are mutant.

To analyze the tail defects during the somitogenesis stages, we placed embryos from mutant crosses at 21°C beginning at the start of gastrulation (shield stage). We routinely use a post-shield stage cooling protocol because it allows us to examine embryos at all somitogenesis stages during the day after fertilization, rather than throughout the night as would occur if embryos were kept at the standard temperature of 28.5°C. Provided the embryos are cooled at shield stage or later, wild-type embryos develop completely normally at temperatures as low as 17°C (Kimelman, 2016a). When we raised embryos from crosses of *hoxa13b*$^{\Delta 16/\Delta 16}$*;hoxd13a*$^{ins13+/-}$ adults at 21°C, we surprisingly observed a high frequency of posterior body defects from mild to severe. To quantify our results, we divided embryos into three classes of defects, with the most severe embryos (class 1) appearing largely identical to embryos with a null mutation in *tbxta*, originally known as *no tail* (*ntl*) mutants (Halpern et al., 1993; Schulte-Merker et al., 1994, Fig. 3A). Interestingly, however, unlike *ntl* mutants that have both a lack of tail and no notochord, our class 1 mutants all contained a notochord (Fig. 3A). Crosses of *hoxa13b*$^{\Delta 16/16}$*;hoxd13a*$^{ins13+/-}$ fish produced a range of embryos from classes 1 to 3 (Fig. 3B, columns 1 and 2). We were able to identify *hoxa13b*$^{\Delta 16/16}$*;hoxd13a*$^{ins13-/-}$ double homozygous mutant males, and these crossed to *hoxa13b*$^{\Delta 16/\Delta 16}$*;hoxd13a*$^{ins13+/-}$ females further enhanced the phenotype (Fig. 3B, column 3). We similarly observed strong defects with crosses of *hoxa13b*$^{\Delta 16/\Delta 16}$*;d13a*$^{ins4+/-}$ and *hoxa13b*$^{\Delta 16/\Delta 16}$*;d13a*$^{\Delta 8+/-}$ fish (Fig. 3B, columns 4 and 5). A cross of the one double homozygous female described above to a double homozygous male produced embryos that were virtually all class 1 and 2 (Fig. 3B, column 6).

We next asked whether the posterior defects were only found in *hoxa13b;d13a* double mutants, or if the same phenotype could be found in *hoxa13b* single mutants kept at 21°C. Embryos from a cross of *hoxa13b*$^{\Delta 16/\Delta 16}$ fish also showed posterior defects at 21°C, although at lower frequencies than with the *hoxa13b;d13a* mutants, and with half the embryos showing a wild-type phenotype (Fig. 3C, column 2, compared to Fig. 3B, columns 1 and 2). Thus, removal of Hoxa13b function results in some posterior defects, but the effect is enhanced when Hoxd13a function is also reduced.

We previously reported that our wild-type stocks of zebrafish contain a naturally occurring variant of Tbxta containing two amino acid changes that lead to a cold-sensitive phenotype (Kimelman, 2016a). Embryos carrying this mutation, which we called *no tail*^{cs} (*ntl*^{cs}), have a completely wild-type phenotype when raised at the standard temperature of 28.5°C, but have the *ntl* null phenotype when raised at 17°C, including a lack of notochord. Because we were seeing cold-sensitive defects in our Hox mutant fish, we wondered whether this mutation might also be present in our Hox mutants, and therefore genotyped the fish described above. All of these fish were found to be homozygous for the *ntl*^{cs} mutation, suggesting that this contributes to the observed phenotype. When we raised homozygous *ntl*$^{cs/cs}$ embryos at 21°C we observed a minor number of posterior defects, but much fewer than found in embryos that were also homozygous for *hoxa13b*$^{\Delta 16}$ (Fig. 3C, columns 1 and 2). Similarly, at 18.5°C the absence of Hoxa13b function enhanced the *ntl*^{cs} phenotype (Fig. 3C, columns 4 and 5). Stronger results were observed at both temperatures when fish that were homozygous for both *hoxa13b*$^{\Delta 16}$ and *ntl*^{cs} and heterozygous for *hoxd13a*^{ins13} were crossed (Fig. 3C, columns 3 and 6). Our results indicate that at 21°C and 18.5°C Tbxta function is only partially reduced in *ntl*^{cs} homozygous embryos, and that removal of Hoxa13b function enhances the strength of the posterior defect, which is further enhanced when Hoxd13a function is also depleted. However, the interaction between *tbxta* and the Hox13 genes is not due to an overall loss of Tbxta function, as the class 1 mutants appear very similar to *ntl* null mutants yet have an intact notochord.

hoxa13b;d13a mutants in a *ntl* wild-type background are hypersensitive to Tbxta reduction

Because the above studies were done in a *ntl*$^{cs/cs}$ background, we backcrossed our *hoxa13b;d13a* double mutant fish into a *ntl* wild-type background. These fish produced normal embryos at both 29°C and 18.5°C, demonstrating that the reduction in Tbxta function produced in *ntl*^{cs} embryos, especially at lower temperatures, is necessary in order to cause posterior defects. To confirm that the reduction in Tbxta is the cause of the posterior defects, we injected wild-type and *hoxa13b;d13a* double mutant embyos in the *ntl* wild-type background with a very low dose (0.2 ng) of a *tbxta* morpholino oligonucleotide that we previously

Development (2020) 147, dev185298. doi:10.1242/dev.185298

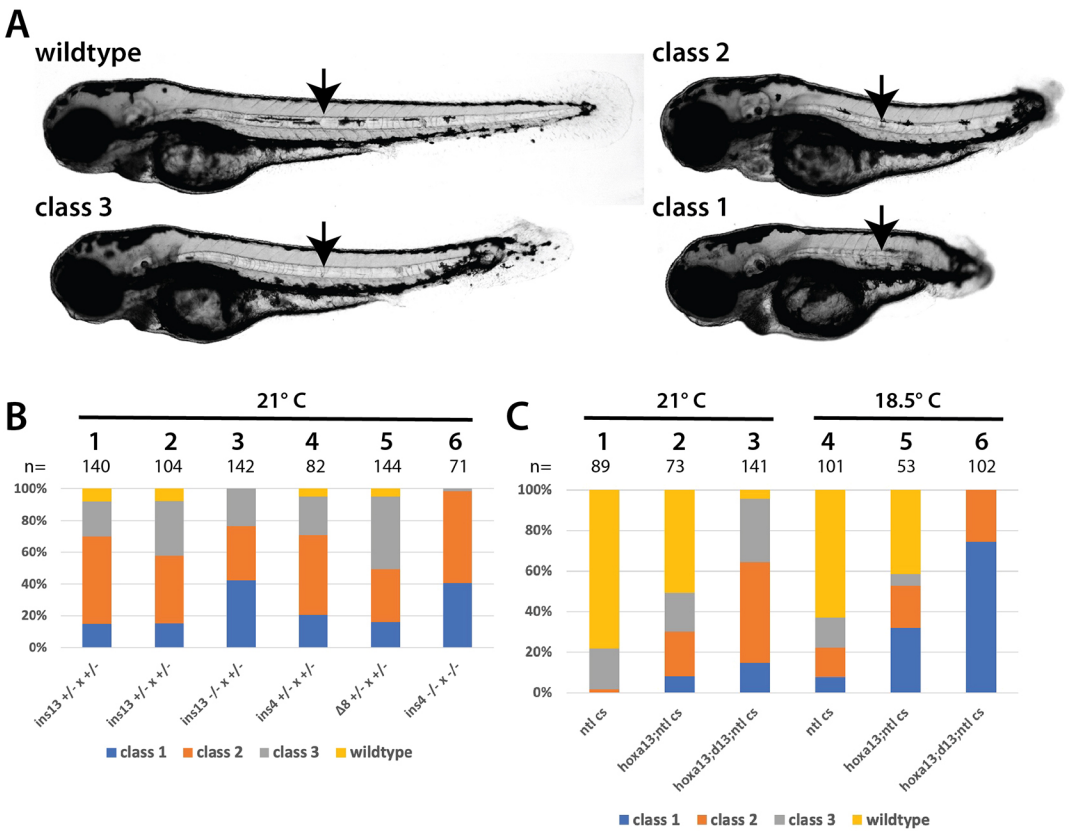

Fig. 3. Interaction between the Hox13 genes and *tbxta*/*ntl*. (A) Classification used to score embryos at 3 dpf. The strongest class, class 1, has the same phenotype as *tbxta*/*ntl* mutants. Class 2 mutants have a clearly truncated axis, and extend beyond the anus at the end of the yolk tube. Class 3 mutants have relatively minor posterior defects. All classes of embryos have a notochord (arrow). (B) Embryos raised from different crosses that were placed at 21°C at shield stage and scored at 3 dpf. The specific *hoxd13a* mutation is shown; all fish were homozygous for both *hoxa13b*$^{\Delta 16}$ and *ntl*^{cs}. The embryos shown in columns 1 and 2 are from two separate families with the same genotype. (C) Embryos raised from different crosses that were placed at 21°C or 18.5°C at shield stage and scored at 3 dpf. The labels for each column refer to the adults used in the cross: *ntl cs*, homozygous for *ntl*^{cs}; *hoxa13;ntl cs*, homozygous for both *hoxa13b*$^{\Delta 16}$ and *ntl*^{cs}; *hoxa13;d13;ntl cs*, homozygous for both *hoxa13b*$^{\Delta 16}$ and *ntl*^{cs}, and heterozygous for *hoxd13a*^{ins13}.

showed specifically phenocopies the *ntl* null mutation at 5 ng (Martin and Kimelman, 2008). We observed a marked hypersensitivity to reduced Tbxta levels when both *hoxa13b* and *hoxd13a* were mutated (Fig. S3). These results further confirm the genetic interaction between the two Hox13 genes and *tbxta*.

Reduction of Tbxta and Hox13 function results in mesodermal deficits

To uncover the cause of the posterior phenotype defects, we examined gene expression using *in situ* hybridization on *hoxa13b*$^{\Delta 16\Delta J16}$;*ntl*$^{cs/cs}$ embryos (hereafter called *hoxa13;ntl*^{cs} embryos) placed at the semi-permissive temperature of 18.5°C from shield stage until mid-somitogenesis. We observed a sharp reduction in the expression of *tbxta* in the NMps in the majority of the *hoxa13;ntl*^{cs} embryos, such that the only expression remaining at the most posterior end of the majority of embryos was *tbxta* expression within the notochord progenitors, which are located just anterior to the NMps (Fig. 4A, gray arrowhead). A strong reduction in *tbxta* was evident in 53.3% of embryos (n=30); the remaining embryos had less reduced or normal expression of *tbxta*. Interestingly, the expression of *tbxta* in the notochord (Fig. 4A, black arrowhead) was normal in all of the *hoxa13;ntl*^{cs} embryos, whereas in *tbxta/ntl* mutants the expression of *tbxta* in the notochord is absent (Schulte-Merker et al., 1994 and see below). The normal *tbxta* expression in the notochord supports our observation that even class 1 embryos have an intact notochord (Fig. 3A), and further supports the idea that the deficit in *hoxa13;ntl*^{cs} embryos at the semi-permissive temperature is specific to the NMps and is not an overall loss of Tbxta function.

Because *tbxta* expression was strongly reduced, we examined other mesodermal markers including *tbx16* and *msgn1*, which mark the initial mesodermal progenitors (Fior et al., 2012; Griffin et al., 1998; Yabe and Takada, 2012), and *pcdh8*, which shows the presomitic mesoderm and nascent somites (Yamamoto et al., 1998). All of these genes were strongly downregulated in the majority of the *hoxa13;ntl*^{cs} embryos (*tbx16*, 65.5%, n=27; *msgn1*, 63.2%, n=19, and *pcdh8*, 55.6%, n=27; Fig. 4H-J). Canonical Wnt signaling is essential both for *brachyury/tbxta* expression and for formation of the mesoderm, and so we examined the two posteriorly expressed canonical Wnt genes, *wnt3a* and *wnt8a*. Both were strongly downregulated in *hoxa13;ntl*^{cs} embryos (*wnt3a*, 89.7%, n=29; *wnt8a*, 90.3%, n=31; Fig. 4B,C). The same mesodermal defects were observed in class 1 *ntl*^{cs} homozygous embryos kept at 18.5°C that were wild type for *hoxa13* and *hoxd13* (Fig. S4), demonstrating that loss of these two genes synergistically enhances the effects of Tbxta reduction. Tailbud Wnt signaling is also regulated by two secreted Wnt inhibitors, Wif1 and Sfrp1a, which are expressed just anterior to the tailbud (Row and Kimelman, 2009). In *hoxa13;ntl*^{cs} embryos, expression of both genes was found to be closer to the posterior end of the embryo, further diminishing the levels of active

Development (2020) 147, dev185298. doi:10.1242/dev.185298

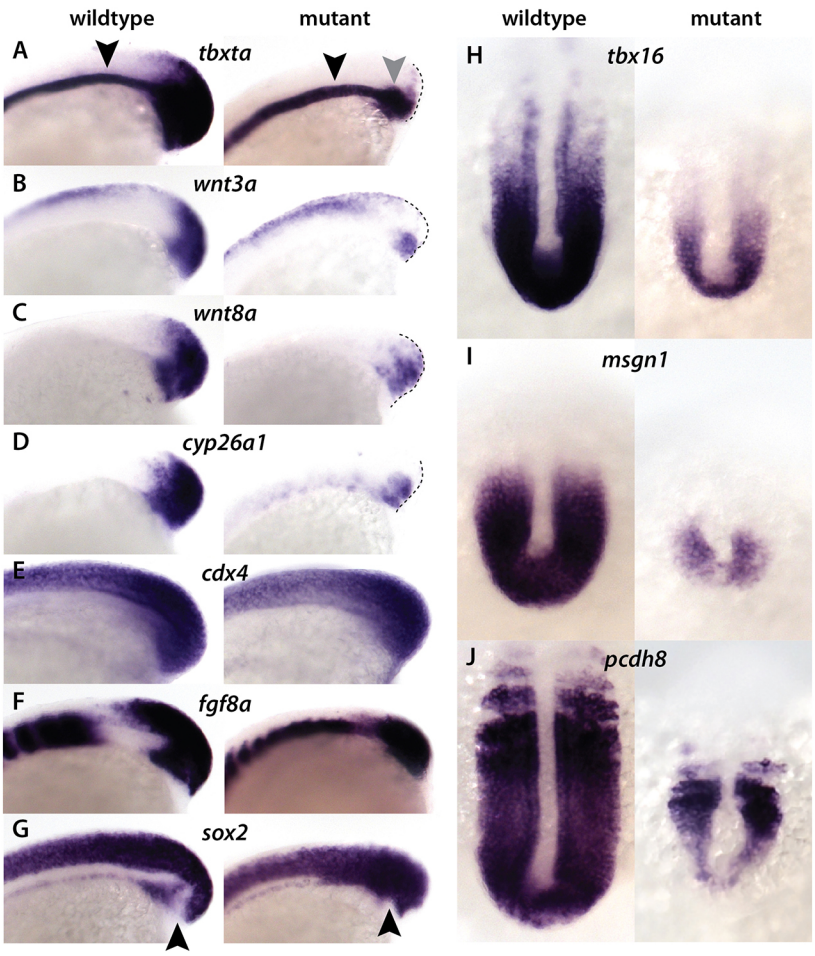

Fig. 4. Mesodermal defects in *hoxa13;ntl*^{cs} embryos maintained at 18.5°C. *In situ* hybridization of 15-somite wild-type and *hoxa13;ntl*^{cs} embryos. (A). In mutant embryos, expression of *tbxta* at the posterior end (NMp domain) of the embryo is absent, whereas expression in the notochord progenitors (gray arrowhead) is retained. Note that in mutant embryos *tbxta* expression in the notochord is normal (black arrowheads). (B-D) Expression of *wnt3a* (B), *wnt8a* (C) and *cyp26a1* (D) are strongly downregulated in the posterior of mutant embryos. (E,F) Expression of *cdx4* (E) and *fgf8a* (F) are largely normal or only partially reduced in the posterior of mutant embryos. (G) *sox2* expression expands into the mesodermal progenitor region in the mutants, whereas in wild-type embryos *sox2* is absent from this region (black arrowheads). (H-J) *tbx16* (H), *msgn1* (I) and *pcdh8* (J) are strongly downregulated in mutant embryos. A-G show side views and H-J show dorsal views.

Wnts (Fig. S5). RA is kept out of the posterior end of the embryo by the Tbxta-regulated degrading enzyme, Cyp26a1, which is essential because RA blocks mesoderm formation (Martin and Kimelman, 2010; Olivera-Martinez et al., 2012; Sive et al., 1990). In *hoxa13;ntl*^{cs} embryos, *cyp26a1 was* also strongly downregulated (88.9%, *n*=27; Fig. 4D). These results indicate that the failure to form mesoderm is a result of loss of canonical Wnt signaling, together with an increase in RA in the posterior of the embryo caused by failure to sustain *cyp26a1* expression.

Although the mesodermal genes were downregulated in *hoxa13;ntl*^{cs} embryos, not all posteriorly expressed genes were affected. For example, *cdx4* and *fgf8a* were normal or only partially reduced (100%, *n*=31 for *cdx4* and *n*=32 for *fgf8a*; Fig. 4E,F). Finally, we examined *sox2* as inhibition of Wnt signaling causes *sox2* to be expressed in the mesodermal region, which we also observed to varying degrees in *hoxa13;ntl*^{cs} embryos (84.6% with expanded *sox2* expression, *n*=26; Fig. 4G). The expansion of *sox2* into the mesodermal region is best seen with fluorescent *in situ* hybridization. In wild-type embryos, *sox2* expression is excluded from the mesodermal progenitors (Martin and Kimelman, 2012) (Fig. S6A-C; Movie 1). In *hoxa13;ntl*^{cs} embryos with a class 1 phenotype, *sox2* expands into this region, filling the entire posterior with *sox2*-positive cells (Fig. S6D-F; Movie 2). This is very similar to that observed in *tbxta/ntl* null mutants and morphants injected with the morpholino oligonucleotide that recapitulates the *ntl* mutant phenotype (Fig. S6G-I; Movie 3), except that in *hoxa13;ntl*^{cs} embryos the notochord was still present, whereas in *tbxta/ntl* null mutants and morphants the notochord was absent (Fig. S6E,H). We also observed the same expansion of neural fate in *hoxa13;ntl*^{cs} embryos with two other neural markers, *sox19a* and *pou5f3* (Fig. S7). In summary, our results show a strong reduction in mesodermal gene expression and a concomitant increase in neural fated cells, exactly as shown for *tbxta/ntl* mutants (Martin and Kimelman, 2012) except that the notochord was unaffected, revealing that the absence of Hoxa13b enhances a reduction in Tbxta activity specifically within the NMps and their mesodermal derivatives.

The defect in *hoxa13;ntl*^{cs} mutant cells is rescued non-cell autonomously

Despite Tbxta having a large number of direct target genes (Garnett et al., 2009; Morley et al., 2009), we previously showed that individual *tbxta/ntl* mutant cells are rescued by the surrounding cells when transplanted into a wild-type environment (Martin and Kimelman, 2008). Thus, although *tbxta/ntl* mutants lack tail mesoderm, transplanted *tbxta/ntl* mutant cells contribute to tail mesoderm, demonstrating that the defect in *tbxta/ntl* is non-cell autonomous. This led to our proposal that the essential role of Brachyury/Tbxta is to control a small number of genes necessary to establish an NMp niche that has high Wnt and low RA, which is essential for mesoderm to form. To compare *hoxa13;ntl*^{cs} cells with *tbxta/ntl* mutant cells, we transplanted 30-50 dye-labeled cells at the start of gastrulation into the future posterior mesodermal region of the embryo, and then let the embryos develop for 2 days at the semi-permissive temperature of 18.5°C. For the *hoxa13;ntl*^{cs} mutants, we only scored transplants in which the donor embryo, which was left to develop after the small number of cells used in transplantation

Development (2020) 147, dev185298. doi:10.1242/dev.185298

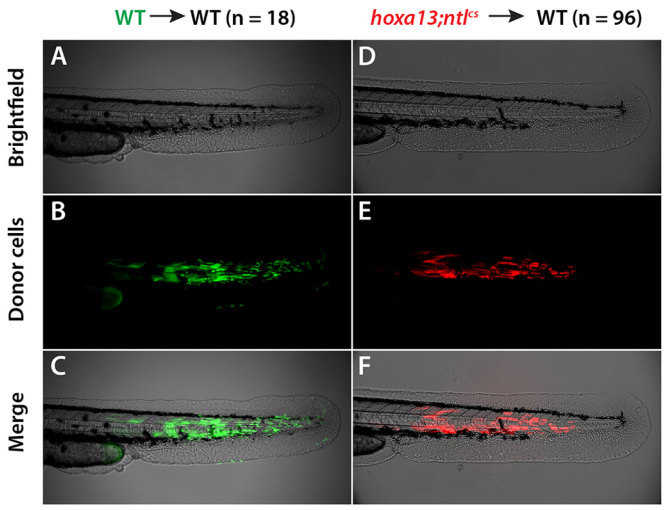

Fig. 5. *hoxa13;ntl*^{cs} cells are rescued for differentiation in a wild-type environment. Donor embryos were injected with a fluorescent dye and then 30-50 cells from each donor were transplanted into the prospective tail mesoderm of a wild-type (WT) host embryo at shield stage. At 2 dpf the embryos were imaged. (A-C) Wild-type donor cells contribute to tail muscle, producing elongated muscle cells within the somites. (D-F) Cells from *hoxa13;ntl*^{cs} donors also contribute to tail muscle.

were removed, developed as a class 1 or class 2 phenotype. Wild-type cells transplanted in this manner ended up in the tail somites as expected (n=18 host embryos scored; Fig. 5A-C;). Similarly, *hoxa13;ntl*^{cs} cells also ended up in the tail somites, appearing indistinguishable from neighboring muscle cells (n=96 host embryos scored; Fig. 5D-F). These results demonstrate that, exactly as with *tbxta/ntl* null cells (Martin and Kimelman, 2008), the defect in *hoxa13;ntl*^{cs} mutants is rescued by the surrounding cells. These results indicate that the absence of Hoxa13b enhances the defect caused by decreased Tbxta function in the NMps, and does not produce additional cell autonomous differentiation defects.

Because overexpression analyses suggested a role for the Hox13 genes in cell movement (Denans et al., 2015; Payumo et al., 2016), we compared cell movements in *hoxa13;ntl*^{cs} cells at the semi-permissive temperature with movements in morphant cells lacking Tbxta. All embryos were injected with a nuclear EGFP then placed at 18.5°C at shield stage. At the 10-somite stage, *hoxa13;ntl*^{cs} embryos that showed a strong posterior phenotype, which would all go on to produce class 1 embryos, were identified and compared with wild-type and *tbxta* morphants by imaging on a confocal microscope. The speed and directionality of cell movements were analyzed as previously described for wild-type embryos (Das et al., 2019; Lawton et al., 2013; Mongera et al., 2018). Interestingly, the overall shape of the tailbud of *hoxa13;ntl*^{cs} embryos was the same as *tbxta* morphant tailbuds, and quite different from a wild-type tailbud (Fig. 6F,I compared to C). To examine the movements in detail, we examined both the NMps and mesodermal progenitor zone (MPZ), which is where *tbx16* and *msgn1* are first activated (Griffin et al., 1998; Yoo et al., 2003). In both regions, the speed of movement and the 'straightness' of movement were similarly reduced in both the *hoxa13;ntl*^{cs} embryos and *tbxta* morphants relative to wild-type embryos (Fig. 6J-M). These results provide further support for the idea that loss of *hoxa13b* enhances a partial reduction in Tbxta function within the NMps and mesodermal progenitors that derive from the NMps, producing defects that appear similar to those seen with a complete loss of Tbxta.

Overexpression of Hox13 proteins is not the opposite of loss of function

Because almost all of the previous studies involved overexpression analysis, we wished to examine the effects of conditionally overexpressing Hoxa13b and Hoxd13a in zebrafish. We produced two transgenic lines that expressed either Hoxa13b or Hoxd13a under the control of a heat-shock (HS) promoter, which allowed us to regulate the timing of transgene expression (*HS:hoxa13b* and *HS:hoxd13a*, respectively). mCherry was co-expressed with the Hox13 proteins in order to identify transgenic lines with strong expression (Fig. 7A). Prior to being heat shocked, embryos were allowed to develop until mid-somitogenesis (10-somite stage) to bypass any possible effects caused by prematurely producing the Hox13 proteins before the stages they are normally expressed. Overexpression of Hoxa13b caused a severe posterior truncation, whereas overexpression of Hoxd13a only caused defects in the anterior of the embryo (Fig. 7B). By quantitatively examining *mCherry* using qPCR, we observed that both transgenic lines produced similar levels of the co-expressed reporter, indicating that the differences were probably not due to differences in expression levels (Fig. 7C). Interestingly, a study in chick that examined cell movement defects caused by Hox13 overexpression found that Hoxa13 caused strong effects, whereas Hoxd13 had no effect (Denans et al., 2015), showing that the effects of overexpression of different Hox13 proteins observed in amniotes are also seen in zebrafish.

Optimally, overexpression causes the opposite effect of loss of function. However, overexpression of transcription factors is potentially problematic because it is possible that, when expressed at higher than endogenous levels, they could bind sites in the DNA that they would not normally bind when expressed at normal levels. Moreover, transcription factors are often in large protein complexes, and overexpression has the potential to create aberrant complexes or disrupt the normal stoichiometry of endogenous complexes. To analyze changes in gene expression caused by overexpression or loss of the Hox13 factors, we isolated tailbud explants from *hoxa13;ntl*^{cs} mutant embryos kept at 18.5°C, as well as tailbud explants from *HS:hoxa13b* embryos, 3 h after a 10 s heat shock, and examined the expression of a selection of genes. In both cases, we cut the explants at the 15-somite stage, selecting for embryos that had a clear morphological defect because these would go on to produce embryos with strong posterior defects, as shown in Fig. 3A and Fig. 7B. To keep the A-P extent of the explants constant, they were all cut to extend from the most posterior end of the embryo to the third most newly formed somite.

In agreement with our *in situ* hybridization data, we observed decreased expression of *tbxta*, *msgn1*, *wnt3a*, *cyp26a1* and *tbx16* in the *hoxa13;ntl*^{cs} mutant embryos, with little to no effect on *cdx4* and *fgf8a* (Fig. 7D). In embryos overexpressing Hoxa13b, we observed decreased expression in most of these genes, including *tbxta*, *wnt3a* and *fgf8a* (Fig. 7D). Importantly, decreased *T/Brachyury* expression was also observed with Hoxa13 overexpression in chick (Denans et al., 2015) and Hoxc13 overexpression in mouse causes a reduction in *wnt3a* levels (Young et al., 2009), demonstrating that our overexpression studies caused similar changes to *brachyury* and Wnt signaling. Comparing the effects of overexpression with loss of function side by side, overexpression of Hoxa13b also caused downregulation of the genes reduced in the *hoxa13;ntl*^{cs} mutant embryos, as well as *fgf8a* and *cdx4*. However, Hoxa13b overexpression did not simply cause an overall decrease in gene expression because other genes, such as *bmp4*, increased under these conditions (Fig. 7D). From these data, we conclude that

Development (2020) 147, dev185298. doi:10.1242/dev.185298

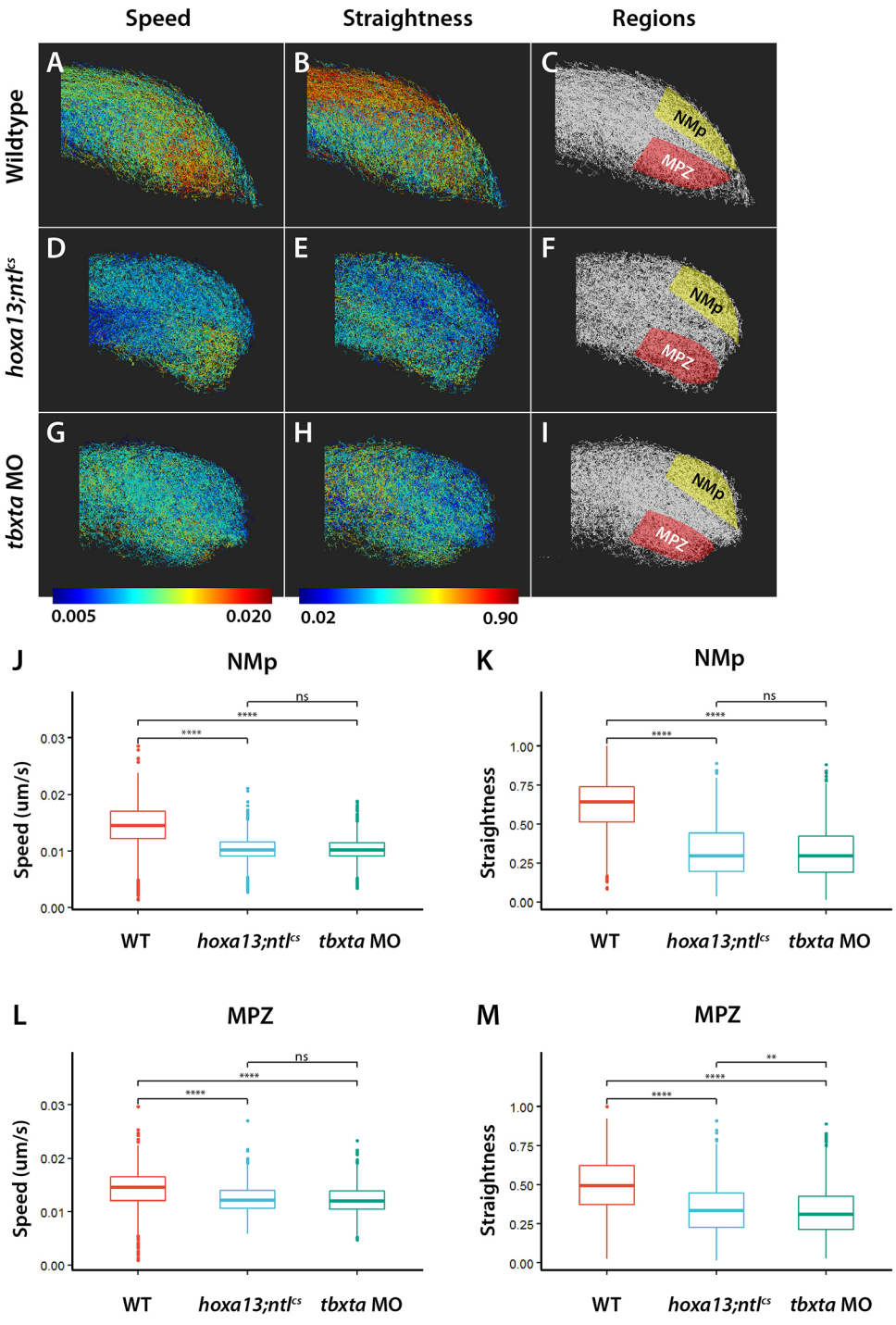

Fig. 6. *hoxa13;ntl*^{cs} mutants and *tbxta* morphants have similar posterior cell movements. (A-I) Embryos expressing nuclear EGFP were filmed at the posterior end. Tracks from a representative embryo are shown in each panel, with the lowest speed or straightness shown in blue and the highest in red. The regions used for quantitative analysis are shown on the right, with the NMps and mesodermal progenitor zone (MPZ) illustrated. Note the similar shapes of the tailbuds of *hoxa13;ntl*^{cs} mutants and *tbxta* morphants (*tbxta* MO) compared with wild type. (J-M) Graphs of speed (J,L) and straightness (K,M) obtained from analysis of 1193, 1295 and 1396 tracks from the NMps and 1173, 1273 and 1399 tracks from the MPZ of three wild-type, *hoxa13;ntlcs* mutant and *tbxta* morphant embryos, respectively. Straightness is the displacement divided by the track length; a value of 1.0 indicates movement in a perfectly straight direction, whereas a value of 0.0 indicates no displacement from the origin. Dunn's test was used for multiple comparisons of mean speed and straightness. ***P*<0.01; *****P*<0.001; ns, no significant difference (*P*>0.05).

overexpression of the Hox13 genes is not simply the opposite of loss of function, suggesting that the effects of Hox13 overexpression need to be interpreted cautiously.

DISCUSSION

Hoxa13b and Hoxd13a cooperate with Brachyury to establish the NMp niche

The Wnt/Brachyury autoregulatory loop is an essential feature of posterior development in early embryonic vertebrate development (Martin and Kimelman, 2008, 2009), with recent evidence from hemichordates demonstrating that it is an ancestral feature of deuterostomes (Fritzenwanker et al., 2019). In vertebrates, this loop ensures that cells remain in a bipotential progenitor state that can produce either neural or mesodermal fates. When canonical Wnt signaling is lost, embryos fail to produce mesoderm and neural tissue increases (Garriock et al., 2015; Gouti et al., 2017, 2014; Jurberg et al., 2014; Martin and Kimelman, 2009; Nowotschin et al., 2012; Wymeersch et al., 2016). Thus, it is crucial that the loop is maintained until the completion of posterior development. Brachyury has a second crucial role in activating *cyp26a1* expression, thus keeping RA levels low at the posterior end of the vertebrate embryo, as high RA inhibits mesoderm formation (Martin and Kimelman, 2010; Olivera-Martinez et al., 2012; Sive et al., 1990). We propose here that the Hox13 genes act to help

Development (2020) 147, dev185298. doi:10.1242/dev.185298

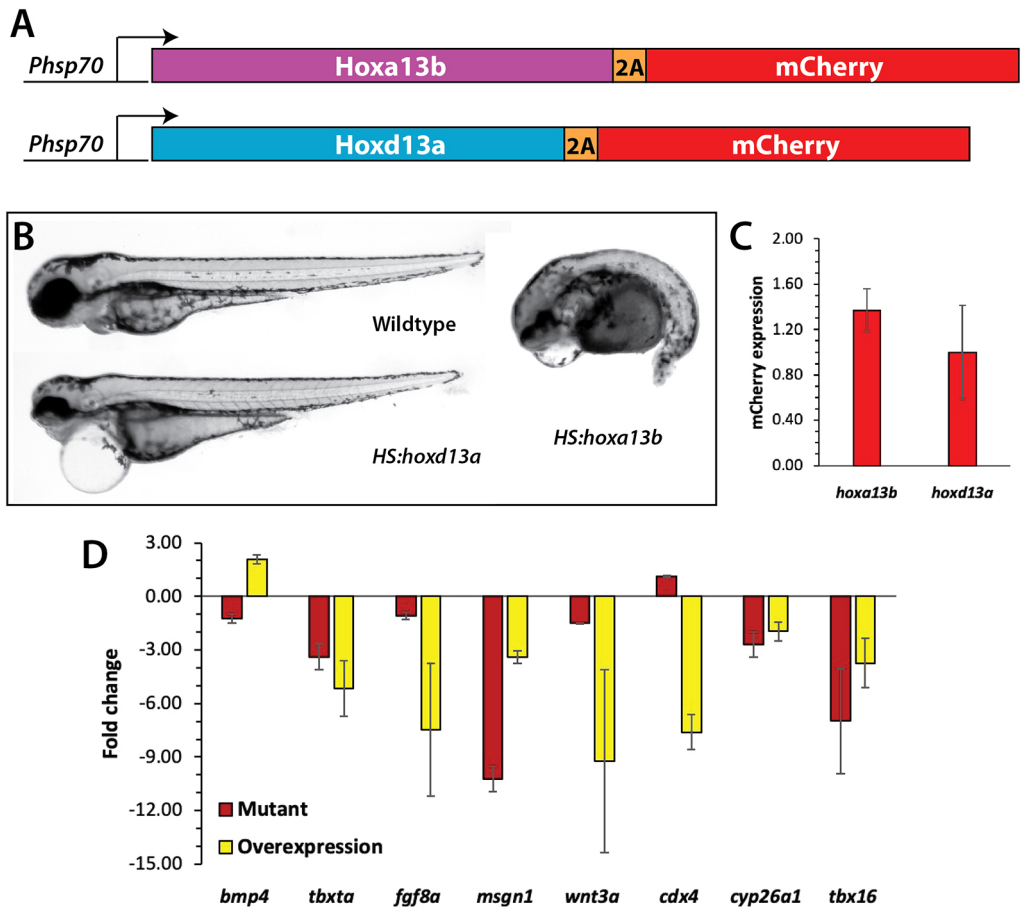

Fig. 7. Analysis of Hox13 overexpression. (A) Constructs used to overexpress Hoxa13b and Hoxd13a. The coding region of each gene was placed under the control of a *hsp70l* promoter, and placed in frame with the 2A peptide and mCherry, which allows both the Hox13 protein and mCherry to be produced as one transcript and two separate proteins. (B) Wild-type and transgenic embryos were heat shocked at the 10-somite stage and then analyzed at 2 dpf. Embryos overexpressing Hoxa13b had posterior truncations, whereas embryos overexpressing Hoxd13a had normal posteriors with minor anterior defects, often including pericardial edema. We observed the same phenotype from Hoxa13b overexpression in $ntl^{+/+}$, $ntl^{cs/+}$ and $ntl^{cs/cs}$ backgrounds. (C) The levels of *mCherry* expression (mean±s.d.) was measured by qPCR in tailbud explants isolated from embryos heat shocked as in B. The differences in *mCherry* expression were not significant (Mann–Whitney test, P=0.4). (D) Fold changes in gene expression in *hoxa13;*ntl^{cs} mutant embryos and embryos overexpressing Hoxa13b. Data from three independent replicates. Only *bmp4* showed opposite effects in the two conditions. *cdx4* in the mutant embryos was unchanged compared with the wild type. Note that the tailbud explants include the posterior notochord and neural tube; thus, the decrease in *tbxta* and *wnt3a* expression in the mutants is not as strong as shown by *in situ* hybridization (Fig. 4) due to their expression in these other tissues.

create a niche at the posterior end of the embryo that has high Wnt and low RA by ensuring that the Wnt/Brachyury loop and Cyp26a1 are robustly expressed throughout much of the somite-forming stages.

Key to our understanding of this pathway is the novel mutation in *tbxta* (ntl^{cs}), which allows us to control Tbxta activity depending on temperature (Kimelman, 2016a). Whereas ntl^{cs} mutants are indistinguishable from wild type at the standard temperature of 28.5°C, when we reduce the temperature to 21°C we begin to see some posterior truncation phenotype, which is further enhanced at 18.5°C. Even at 18.5°C, less than 10% of the embryos show the *ntl* null phenotype. This sensitized background was very useful for exploring the Hox13 mutants because the percentage of embryos with perturbed phenotypes increased in embryos homozygous for a loss of *hoxa13b*, and even more so when *hoxd13a* was also mutant. Possibly, the number of embryos with severe posterior truncations will increase yet further when the other less highly expressed posterior Hox13 genes (*hoxa13a*, *hoxc13a* and *hoxc13b*) are also mutant.

Although the Hox13 genes have been proposed to act to terminate axis extension, we find that they are expressed very early in somitogenesis, with *hoxa13b* expressed at the start of somitogenesis and *hoxd13a* expressed at the eight-somite stage, which seems surprising for their proposed role in terminating the axis. Similarly, a quantitative analysis in mouse has shown that Hox13 genes are activated at E9.5 in the neuromesodermal progenitor region, whereas somitogenesis does not end until 4 days later (Wymeersch et al., 2019). In chick embryos, strong expression of the Hox13 genes, as shown by *in situ* hybridization, was reported to begin around halfway through somitogenesis (Denans et al., 2015). Although the timing of onset does not preclude the possibility that the Hox13 genes are involved in axis termination, their early expression at least raises the possibility of alternative roles.

The evidence for Hox13 genes as axis terminators is based almost entirely on overexpression studies, with the one exception being the mouse *Hoxb13* mutant, which adds two somites to the tip of the tail, thus increasing the body from 65 to 67 somites, through enhanced proliferation and decreased cell death in the mesoderm and neural ectoderm (Economides et al., 2003), whereas all other Hox13 mutants show no effect on axis length (Dolle et al., 1993; Fromental-Ramain et al., 1996; Godwin and Capecchi, 1998;

Development (2020) 147, dev185298. doi:10.1242/dev.185298

Suemori and Noguchi, 2000). Interestingly, the one zebrafish *hoxb13* gene, *hoxb13a*, is not expressed in the tailbud, and so perhaps the regulation of tailbud proliferation and apoptosis by *Hoxb13* is an amniote or mammalian adaptation.

Although overexpression is commonly and often successfully used to study the role of different proteins in embryonic development, it can also lead to artifacts, particularly because transcription factors at higher than endogenous levels could bind to aberrant binding sites in the genome. Moreover, as many transcription factors act in protein complexes, overexpression has the potential to disrupt the normal stoichiometry of the complex. In our overexpression studies using temporally controllable heat shock lines, we saw strong effects on embryonic posterior development when we overexpressed *hoxa13b*. Similarly, a previous study in zebrafish that mosaically overexpressed *hoxa13b* using a promoter that restricted expression to the mesodermal progenitors and their descendants also observed defects in posterior development (Payumo et al., 2016), in agreement with our results. Why *hoxd13a* overexpression does not cause strong posterior defects is not yet clear, although it is in line with observations from overexpression studies in chick that also showed strong effects from *Hoxa13* overexpression but no effect from *Hoxd13* overexpression (Denans et al., 2015). Although the DNA binding regions of the different Hox13 factors (the homeobox) are very highly conserved, the N terminus, which makes up almost all of the rest of the protein, is quite different between Hoxa13 and Hoxd13 proteins.

The most important finding from our overexpression studies is that in most cases the regulation of gene expression by overexpression is not the opposite of loss of function, raising concerns about the interpretation of overexpression studies of the Hox13 proteins. As previously reported in mouse for *Hoxc13* overexpression (Young et al., 2009), we see a partial reduction in *wnt3a* expression when Hoxa13b is overexpressed, and a downregulation of *tbxta* expression under these conditions, in agreement with the reduction in *T/Brachyury* observed in chick embryos when *Hoxa13* is overexpressed (Denans et al., 2015). Thus, our overexpression results parallel those reported in amniotes. However, we also see a reduction in *tbxta* and *wnt3a* in the *hoxa13; ntl*^{cs} mutant embryos at the semi-permissive temperature of 18.5°C, demonstrating that the Hox13 genes promote the expression of these genes (and others), rather than inhibiting them. We therefore suggest that the previous overexpression studies should be carefully interpreted.

A new model for the role of the Hox13 genes

We propose that one key role of the Hox13 genes is to provide robustness to the Wnt/Brachyury loop because it is crucial that this loop is strongly expressed throughout all of the somitogenesis stages to ensure that mesoderm can be produced from the NMps as the body extends (Fig. 8). If the loop fails at any point during somitogenesis as a result of decreased Wnt or Brachyury, then the NMps fail to produce the somites and neural fates increase because only the *sox2*-positive derivatives of the NMps are produced (Garriock et al., 2015; Gouti et al., 2014; Martin and Kimelman, 2012; Tsakiridis et al., 2014; Turner et al., 2014). Wnt signaling is crucial for activation of downstream genes, particularly *tbx16* in zebrafish and *Tbx6* and *Msgn1* in mice (Bouldin et al., 2015; Chalamalasetty et al., 2014; Kimelman, 2016b; Nowotschin et al., 2012; Wittler et al., 2007). These downstream genes act to inhibit the NMp state and to activate subsequent genes needed for somite formation (Fig. 8). A second important role of Brachyury is to activate expression of the RA-degrading enzyme Cyp26a1 (Martin and Kimelman, 2010), which keeps the levels of RA low in the NMps as increased RA levels terminate axis extension. Although RA is not necessary in mice or zebrafish for terminating axis extension (Berenguer et al., 2018; Cunningham et al., 2011), it is essential that the levels in the posterior end of the embryo are kept very low (Martin and Kimelman, 2010; Olivera-Martinez et al., 2012; Sive et al., 1990).

The regulation of Wnt signaling in the tailbud is challenging for the embryo. In the NMps, Wnt signaling needs to be regulated at a level high enough for Brachyury expression to be maintained, but not so high as to force the cells into a mesodermal fate. Once the cells exit the most posterior end of the embryo and enter the posterior presomitic mesoderm, they are exposed to higher Wnt levels than found in the NMp zone, which then activates mesodermal gene expression (Bouldin et al., 2015, Fig. 8). However, if Wnt is too high throughout the tailbud it produces deleterious effect such as suppressed neural development (Jurberg et al., 2014; Garriock et al., 2015; Martin and Kimelman, 2012)

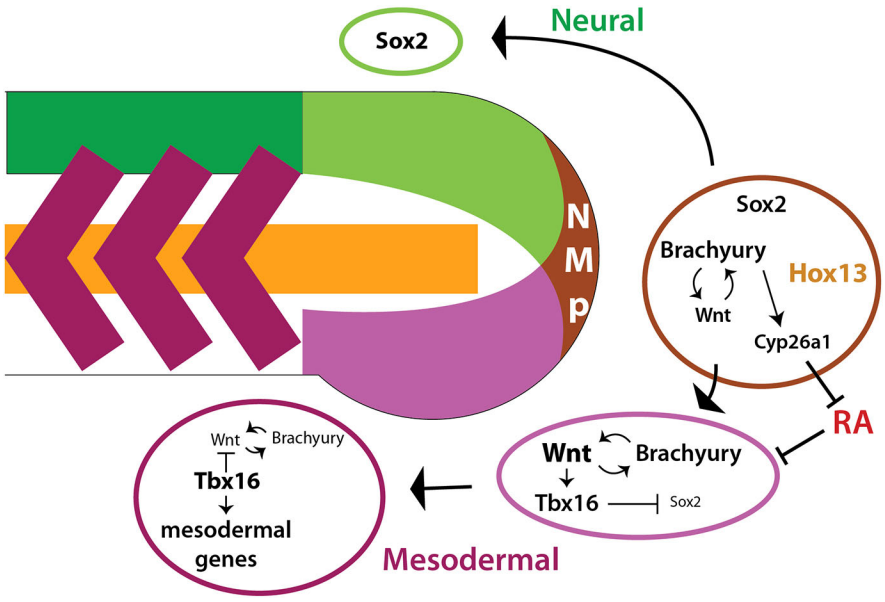

Fig. 8. Model for formation of neural and mesodermal tissues from the NMps. A model based on work presented here and from other studies. The NMps co-express Sox2 and Brachyury/Tbxta. Cells that migrate into a Wnt-free environment retain Sox2 expression and differentiate as neural cells. Cells that enter a high Wnt environment retain Brachyury expression and activate Tbx16 (Tbx6 in amniotes), which together with Msgn1 and Tbx16l (Morrow et al., 2017) activates mesodermal gene expression. Tbx16 also represses both Sox2 and later Wnt, to promote mesodermal differentiation (Bouldin et al., 2015). Brachyury has an essential role in creating the niche for mesoderm formation by activating canonical Wnt expression and inhibiting RA from the posterior end by inducing the expression of Cyp26a1. We propose that the Hox13 proteins act within the NMps to enhance the niche-promoting effects of Brachyury.

Development (2020) 147, dev185298. doi:10.1242/dev.185298

and aberrant segmentation (Bajard et al., 2014; Garriock et al., 2015; Jurberg et al., 2014). Thus, the role of the Hox13 genes might be to sustain the Wnt/Brachyury loop in the most posterior end of the embryo at a low level that is just sufficient to maintain Brachyury expression, but not so high as to cause deleterious effects.

How then might the Hox13 proteins regulate the Wnt/Brachyury loop? An intriguing possibility is suggested from a study in *Caenorhabditis elegans* that Hox factors act to ensure robust gene expression by consistently promoting the full activation of target genes by other transcription factors, and as such have been termed 'guarantors' of gene expression (Zheng and Chalfie, 2016; Zheng et al., 2015). In the guarantor model, the Hox proteins are not absolutely required for target gene expression and instead are crucial in cases where some cells or groups of cells fall below a critical threshold of expression of an essential gene because of variability in levels of transcription. In this sense, the variable and relatively low level of posterior embryonic defects seen at the fully permissive temperature (29°C) in our cross of double mutant fish in the $ntl^{cs/cs}$ background can be viewed as embryos that stochastically fall on the lower end of expression of the Wnt/Brachyury loop due to very minor reductions in Tbxta activity without the help of the Hox13 factors to boost the levels. When Tbxta activity is further reduced in these embryos by lowering the temperature, the number of embryos that stochastically fall below the necessary threshold to sustain the loop increases, resulting in a greater number of embryos with a posterior defect. Although a true test of this model requires eliminating all five tailbud-expressed Hox13 genes in zebrafish, the results suggest that even a complete loss of Hox13 function may only be a partially penetrant effect with regards to completion of the A-P axis.

Which genes are regulated by the Hox13 factors in any system remains unknown but, in zebrafish, *tbxta/brachyury* is an intriguing candidate as it is upstream of both the *wnt* genes and *cyp26a1* (Martin and Kimelman, 2008, 2010), and its expression is strongly downregulated in the $hoxa13;ntl^{cs}$ embryos at the semi-permissive temperature (Fig. 4). Interestingly, a DNA fragment containing just 2.1 kb upstream of the *tbxta* start site produced *tbxta* expression throughout the mesoderm during the gastrula stages, and later expression in the notochord, but it did not activate tailbud *tbxta* expression, demonstrating that proximal sequences of *tbxta* do not activate expression in the NMps during the somitogenesis stages (Harvey et al., 2010). Importantly, using a new method for identifying *in vivo* Hox13 binding sites in tailbud cells has led to identification of a somitogenesis stage tailbud enhancer for *tbxta*, providing one clear locus of Hox13 regulation of the Wnt/Brachyury loop (Z.Y., C. R. Braden, A. E. Wills and D.K. unpublished).

MATERIALS AND METHODS

Mutants

Wild-type fish were an AB/WIK mixture. Fish were used for crosses at ages between 3 months and 3 years. The ntl^{cs} mutant fish (*ntla w181*) has been described previously (Kimelman, 2016a).

In the $ntl^{cs};hoxa13b^{\Delta 16}$ mutant (designated as line w243), 20 bp were deleted and 4 bp were added resulting in a 16 bp deletion. In the *hoxa13b* sequence, CCCAAGTCCTGCACGCAACCCACCACATATGG was changed to CCCAAGagaaATATGG, with the lower case letters indicating novel bases.

In the $ntl^{cs};\ hoxa13b^{\Delta 16;}\ hoxd13a^{ins13}$ mutant (designated as line w244), 13 bp were inserted. In the *hoxd13a* sequence, CCCGTGGACCAC was changed to CCCGTGaagcctcggtgaaGACCAC, with the lower case letters indicating novel bases.

In the $ntl^{cs};\ hoxa13b^{\Delta 16};\ hoxd13a^{ins4}$ mutant (designated as line w245), 2 bp were deleted and 6 bp were added, resulting in a 4 bp insertion. In the *hoxd13a* sequence, AACCCGTGGACCAC was changed to AACCCGcc-aataGACCAC, with the lower case letters indicating novel bases.

In the $ntl^{cs};\ hoxa13b^{\Delta 16;}\ hoxd13a^{\Delta 8}$ mutant (designated as line w246), 8 bp were deleted. In the *hoxd13a* sequence, CAATAAACCCGTGGAC-CACGG was changed to CAATAAACCACGG.

All CRISPR mutant lines were designed and produced following published methods (Moreno-Mateos et al., 2015; Talbot and Amacher, 2014). The sequence used to make a gRNA for *hoxa13b* was GGGGGTTGCGTGCAGGACTT, which has a base change at the second base to allow for synthesis by T7 polymerase. The sequence used to make a guide RNA (gRNA) for *hoxd13a* was GGGGCTTCACCGTGGTCCAC, which has a base change at the second base to allow for synthesis by T7 polymerase.

Transgenic lines

The *hoxa13b* and *hoxd13a* coding regions were amplified from 15-somite stage zebrafish embryo cDNA and inserted into a vector such that the stop codons were removed and a viral 2A peptide (Provost et al., 2007) was placed immediately after the coding region. The mCherry sequence was placed immediately after the 2A sequence. This sequence was placed in a Tol2-*hsp70* vector and the resulting plasmid was used together with Tol2 transposase to create stable transgenic lines as previously described (Kawakami, 2004): *hsp70l:hoxa13b-2A-mCherry* (designated w247) and *hsp70l:hoxd13a-2A-mCherry* (designated w248). Transgenic lines were heat shocked at 40°C for 30 min.

All animal protocols used here were approved by the University of Washington Institutional Animal Care and Use Committee.

In situ hybridization

Alkaline phosphate *in situ* hybridization used standard conditions (https://wiki.zfin.org/display/prot/Thisse+Lab+-+In+Situ+Hybridization+Protocol+-+2010+update). Fluorescent *in situ* hybridization used a published procedure (Lauter et al., 2011).

Morpholino oligonucleotide

The sequence and use of the *tbxta/ntl* morpholino has been previously described (Martin and Kimelman, 2008). Injected at 5 ng, it completely recapitulates the *ntl* mutant phenotype.

Cell transplantation

Embryos were injected at the one-cell stage with 2% fluorescein or rhodamine dextran, and transplanted into the ventral side of a shield stage wild-type embryo using a CellTram (Eppendorf). The $hoxa13;ntl^{cs}$ donor embryos were also raised after a small number of cells were taken for transplantation and only donors that produced a strong phenotype were scored.

qPCR on tailbud explants

HS:hoxa13b and *HS:hoxd13a* embryos were heat shocked at the 10-somite stage and kept at 28.5°C until they reached the 15-somite stage (about 3 h post heat shock). The $hoxa13;ntl^{cs}$ embryos were placed at 18.5°C at shield stage and kept at this temperature until sampling. Embryos were sorted either by mCherry expression for the transgenic embryos or by phenotype (large neural tube and small presomitic mesoderm) for the mutants. Wild-type control embryos were manipulated the same way for each treatment. Tailbuds were isolated at the 15-somite stage using the method we described previously (Manning and Kimelman, 2015) in which the epidermis is removed prior to cutting the explant. The explants began at the boundary of the third most newly formed somite and extended to the most posterior end of the embryo. Thirty tailbuds were sampled and pooled for RNA extraction from each group. RNA was extracted using TriReagent (Invitrogen) and purified with RNA Clean & Concentrator spin columns (Zymo Research). cDNA was produced using the iScript Supermix cDNA kit (BioRad). Quantitative PCR was performed in triplicate using the SsoAdvanced Universal SYBR Green Supermix kit (BioRad) on a CFX Connect Real-Time PCR Detection System

(BioRad). The primers used for amplification are listed in Table S1. The level of each specific gene in the explant was normalized to the level of *ribosomal 18S* mRNA in the explant, and the fold change of gene expression due to treatment (overexpression or mutation of *hoxa13b*) was calculated according to published methods (Schmittgen and Livak, 2008).

Cell tracking

Embryos were injected with 50 ng mRNA encoding H2B-EGFP synthesized *in vitro* from the plasmid CS2-H2B-EGFP using the mMESSAGE MACHINE SP6 kit (ThermoFisher). Wild-type, *hoxa13;ntl^{cs}* and *tbxta* morphant embryos were placed at 18.5°C at shield stage and kept at this temperature until filming at the 10-somite stage. Embryos were mounted in 1% low-melt agarose and imaged using a spinning disk confocal microscope [inverted Marianas spinning disk system (Intelligent Imaging Innovations, 3i) with an Evolve 10 MHz EMCCD camera (Photometrics) and a Zeiss microscope Plan-NEOFLUAR 25×0.8 immersion objective]. Time-lapse image stacks with a step size of 2 µm were taken every 2 min for a period of 2 h at 25°C. The *hoxa13;ntl^{cs}* and *tbxta* morphant embryos were retrieved from the agarose after imaging and allowed to develop to 2 dpf (days post-fertilization) at 18.5°C to confirm phenotype. Three embryos from each genotype were used for cell movement analysis using Imaris (Oxford Instruments).

Quantification and statistical analysis

The Mann–Whitney test was used for comparison of the qPCR results for *mCherry* expression in the explants of *HS:hoxa13b* and *HS:hoxd13a* embryos after heat shock. Fisher's exact test was used to compare the number of defective embryos (class 1, 2 and 3 phenotypes pooled) after injection of 0.2 ng *tbxta* morpholino in the wild-type and *hoxa13;d13* mutant fish in a *ntl$^{+/+}$* background.

For the cell movement data analysis, only tracks with a duration longer than 30 min were included. The mean track speed and straightness were calculated using Imaris. Tracks were color-coded by mean track speed or straightness using Imaris to generate Fig. 6A,B,D,E,G,H. From each embryo, 300 to 500 representative tracks were manually and randomly picked from the NMp and MPZ based on the physical position. Tracks from the same region (NMp or MPZ) of three embryos were pooled for each genotype for statistical analysis of cell movement. Dunn's test was used for the post hoc multiple comparisons of cell moving speed and straightness after detection of significant difference using the Kruskal–Wallis test. All statistical analyses were conducted using R 3.6.0. The significance level was set at $P<0.05$.

Acknowledgements

We thank Natalie Smith and Adrian Wang for critical comments on the manuscript, Eric Thomas and Andrew Curtwright for advice on CRISPR, and Natalie Smith for invaluable help throughout this project.

Competing interests

The authors declare no competing or financial interests.

Author contributions

Conceptualization: Z.Y., D.K.; Methodology: Z.Y., D.K.; Validation: Z.Y., D.K.; Investigation: Z.Y., D.K.; Writing - original draft: D.K.; Writing - review & editing: Z.Y., D.K.; Visualization: Z.Y., D.K.; Supervision: D.K.; Project administration: D.K.; Funding acquisition: D.K.

Funding

D.K. was supported by a grant from the National Institutes of Health (RO1GM079203). Deposited in PMC for release after 12 months.

Supplementary information

Supplementary information available online at https://dev.biologists.org/lookup/doi/10.1242/dev.185298.supplemental

Peer review history

The peer review history is available online at https://dev.biologists.org/lookup/doi/10.1242/dev.185298.reviewer-comments.pdf

References

Aires, R., de Lemos, L., Novoa, A., Jurberg, A. D., Mascrez, B., Duboule, D. and Mallo, M. (2019). Tail bud progenitor activity relies on a network comprising Gdf11, Lin28, and Hox13 genes. *Dev. Cell* **48**, 383-395.e388. doi:10.1016/j.devcel.2018.12.004

Amin, S., Neijts, R., Simmini, S., van Rooijen, C., Tan, S. C., Kester, L., van Oudenaarden, A., Creyghton, M. P. and Deschamps, J. (2016). Cdx and T brachyury co-activate growth signaling in the embryonic axial progenitor niche. *Cell Rep* **17**, 3165-3177. doi:10.1016/j.celrep.2016.11.069

Bajard, L., Morelli, L. G., Ares, S., Pecreaux, J., Julicher, F. and Oates, A. C. (2014). Wnt-regulated dynamics of positional information in zebrafish somitogenesis. *Development* **141**, 1381-1391. doi:10.1242/dev.093435

Berenguer, M., Lancman, J. J., Cunningham, T. J., Dong, P. D. S. and Duester, G. (2018). Mouse but not zebrafish requires retinoic acid for control of neuromesodermal progenitors and body axis extension. *Dev. Biol.* **441**, 127-131. doi:10.1016/j.ydbio.2018.06.019

Bouldin, C. M., Manning, A. J., Peng, Y.-H., Farr, G. H. I., Hung, K. L., Dong, A. and Kimelman, D. (2015). Wnt signaling and tbx16 form a bistable switch to commit bipotential progenitors to mesoderm. *Development* **142**, 2499-2507. doi:10.1242/dev.124024

Chalamalasetty, R. B., Garriock, R. J., Dunty, W. C., Jr., Kennedy, M. W., Jailwala, P., Si, H. and Yamaguchi, T. P. (2014). Mesogenin 1 is a master regulator of paraxial presomitic mesoderm differentiation. *Development* **141**, 4285-4297. doi:10.1242/dev.110908

Cunningham, T. J., Zhao, X. and Duester, G. (2011). Uncoupling of retinoic acid signaling from tailbud development before termination of body axis extension. *Genesis* **49**, 776-783. doi:10.1002/dvg.20763

Das, D., Julich, D., Schwendinger-Schreck, J., Guillon, E., Lawton, A. K., Dray, N., Emonet, T., O'Hern, C. S., Shattuck, M. D. and Holley, S. A. (2019). Organization of embryonic morphogenesis via mechanical information. *Dev. Cell* **49**, 829-839.e825. doi:10.1016/j.devcel.2019.05.014

Denans, N., Iimura, T. and Pourquié, O. (2015). Hox genes control vertebrate body elongation by collinear Wnt repression. *Elife* **4**, e04379. doi:10.7554/eLife.04379.031

Dolle, P., Dierich, A., LeMeur, M., Schimmang, T., Schuhbaur, B., Chambon, P. and Duboule, D. (1993). Disruption of the Hoxd-13 gene induces localized heterochrony leading to mice with neotenic limbs. *Cell* **75**, 431-441. doi:10.1016/0092-8674(93)90378-4

Economides, K. D., Zeltser, L. and Capecchi, M. R. (2003). Hoxb13 mutations cause overgrowth of caudal spinal cord and tail vertebrae. *Dev. Biol.* **256**, 317-330. doi:10.1016/S0012-1606(02)00137-9

Fior, R., Maxwell, A. A., Ma, T. P., Vezzaro, A., Moens, C. B., Amacher, S. L., Lewis, J. and Saude, L. (2012). The differentiation and movement of presomitic mesoderm progenitor cells are controlled by Mesogenin 1. *Development* **139**, 4656-4665. doi:10.1242/dev.078923

Fritzenwanker, J. H., Uhlinger, K. R., Gerhart, J., Silva, E. and Lowe, C. J. (2019). Untangling posterior growth and segmentation by analyzing mechanisms of axis elongation in hemichordates. *Proc. Natl. Acad. Sci. USA* **116**, 8403-8408. doi:10.1073/pnas.1817496116

Fromental-Ramain, C., Warot, X., Messadecq, N., LeMeur, M., Dolle, P. and Chambon, P. (1996). Hoxa-13 and Hoxd-13 play a crucial role in the patterning of the limb autopod. *Development* **122**, 2997-3011.

Garnett, A. T., Han, T. M., Gilchrist, M. J., Smith, J. C., Eisen, M. B., Wardle, F. C. and Amacher, S. L. (2009). Identification of direct T-box target genes in the developing zebrafish mesoderm. *Development* **136**, 749-760. doi:10.1242/dev.024703

Garriock, R. J., Chalamalasetty, R. B., Kennedy, M. W., Canizales, L. C., Lewandoski, M. and Yamaguchi, T. P. (2015). Lineage tracing of neuromesodermal progenitors reveals novel Wnt-dependent roles in trunk progenitor cell maintenance and differentiation. *Development* **142**, 1628-1638. doi:10.1242/dev.111922

Godwin, A. R. and Capecchi, M. R. (1998). Hoxc13 mutant mice lack external hair. *Genes Dev.* **12**, 11-20. doi:10.1101/gad.12.1.11

Gouti, M., Tsakiridis, A., Wymeersch, F. J., Huang, Y., Kleinjung, J., Wilson, V. and Briscoe, J. (2014). In vitro generation of neuromesodermal progenitors reveals distinct roles for wnt signalling in the specification of spinal cord and paraxial mesoderm identity. *PLoS Biol.* **12**, e1001937. doi:10.1371/journal.pbio.1001937

Gouti, M., Metzis, V. and Briscoe, J. (2015). The route to spinal cord cell types: a tale of signals and switches. *Trends Genet.* **31**, 282-289. doi:10.1016/j.tig.2015.03.001

Gouti, M., Delile, J., Stamataki, D., Wymeersch, F. J., Huang, Y., Kleinjung, J., Wilson, V. and Briscoe, J. (2017). A Gene regulatory network balances neural and mesoderm specification during vertebrate trunk development. *Dev. Cell* **41**, 243-261.e247. doi:10.1016/j.devcel.2017.04.002

Griffin, K. J., Amacher, S. L., Kimmel, C. B. and Kimelman, D. (1998). Molecular identification of spadetail: regulation of zebrafish trunk and tail mesoderm formation by T-box genes. *Development* **125**, 3379-3388.

Halpern, M. E., Ho, R. K., Walker, C. and Kimmel, C. B. (1993). Induction of muscle pioneers and floor plate is distinguished by the zebrafish no tail mutation. *Cell* **75**, 99-111. doi:10.1016/S0092-8674(05)80087-X

Harvey, S. A., Tumpel, S., Dubrulle, J., Schier, A. F. and Smith, J. C. (2010). no tail integrates two modes of mesoderm induction. *Development* **137**, 1127-1135. doi:10.1242/dev.046318
Henrique, D., Abranches, E., Verrier, L. and Storey, K. G. (2015). Neuromesodermal progenitors and the making of the spinal cord. *Development* **142**, 2864-2875. doi:10.1242/dev.119768
Holley, S. A. (2007). The genetics and embryology of zebrafish metamerism. *Dev. Dyn.* **236**, 1422-1449. doi:10.1002/dvdy.21162
Jurberg, A. D., Aires, R., Novoa, A., Rowland, J. E. and Mallo, M. (2014). Compartment-dependent activities of Wnt3a/β-catenin signaling during vertebrate axial extension. *Dev. Biol.* **394**, 253-263. doi:10.1016/j.ydbio.2014.08.012
Kawakami, K. (2004). Transgenesis and gene trap methods in zebrafish by using the Tol2 transposable element. *Methods Cell Biol.* **77**, 201-222. doi:10.1016/S0091-679X(04)77011-9
Kimelman, D. (2016a). A novel cold-sensitive mutant of ntla reveals temporal roles of brachyury in zebrafish. *Dev. Dyn.* **245**, 874-880. doi:10.1002/dvdy.24417
Kimelman, D. (2016b). Tales of tails (and trunks): forming the posterior body in vertebrate embryos. *Curr. Topics in Dev. Biol.* **116**, 517-536. doi:10.1016/bs.ctdb.2015.12.008
Kimelman, D. and Martin, B. L. (2012). Anterior-Posterior patterning in early development: three stratagies. *WIREs Dev. Biol.* **1**, 253-266. doi:10.1002/wdev.25
Kimelman, D., Smith, N. L., Lai, J. K. H. and Stainier, D. Y. (2017). Regulation of posterior pody and epidermal morphogenesis in zebrafish by localized Yap1 and Wwtr1. *eLife* **6**, e31065. doi:10.7554/eLife.31065
Lauter, G., Söll, I. and Hauptmann, G. (2011). Multicolor fluorescent in situ hybridization to define abutting and overlapping gene expression in the embryonic zebrafish brain. *Neural Dev.* **6**, 10. doi:10.1186/1749-8104-6-10
Lawton, A. K., Nandi, A., Stulberg, M. J., Dray, N., Sneddon, M. W., Pontius, W., Emonet, T. and Holley, S. A. (2013). Regulated tissue fluidity steers zebrafish body elongation. *Development* **140**, 573-582. doi:10.1242/dev.090381
Ma, Z., Zhu, P., Shi, H., Guo, L., Zhang, Q., Chen, Y., Chen, S., Zhang, Z., Peng, J. and Chen, J. (2019). PTC-bearing mRNA elicits a genetic compensation response via Upf3a and COMPASS components. *Nature* **568**, 259-263. doi:10.1038/s41586-019-1057-y
Mallo, M. (2018). Reassessing the role of Hox genes during vertebrate development and evolution. *Trends Genet.* **34**, 209-217. doi:10.1016/j.tig.2017.11.007
Manning, A. J. and Kimelman, D. (2015). Tbx16 and Msgn1 are required to establish directional cell migration of zebrafish mesodermal progenitors. *Dev. Biol.* **406**, 172-185. doi:10.1016/j.ydbio.2015.09.001
Martin, B. L. (2016). Factors that coordinate mesoderm specification from neuromesodermal progenitors with segmentation during vertebrate axial extension. *Semin. Cell Dev. Biol.* **49**, 59-67. doi:10.1016/j.semcdb.2015.11.014
Martin, B. L. and Kimelman, D. (2008). Regulation of canonical Wnt signaling by Brachyury is essential for posterior mesoderm formation. *Dev. Cell* **15**, 121-133. doi:10.1016/j.devcel.2008.04.013
Martin, B. L. and Kimelman, D. (2009). Wnt signaling and the evolution of embryonic posterior development. *Curr. Biol.* **19**, R215-R219. doi:10.1016/j.cub.2009.01.052
Martin, B. L. and Kimelman, D. (2010). Brachyury establishes the embryonic mesodermal progenitor niche. *Genes Dev.* **24**, 2778-2783. doi:10.1101/gad.1962910
Martin, B. L. and Kimelman, D. (2012). Canonical Wnt signaling dynamically controls multiple stem cell fate decisions during vertebrate body formation. *Dev. Cell* **22**, 223-232. doi:10.1016/j.devcel.2011.11.001
Mongera, A., Rowghanian, P., Gustafson, H. J., Shelton, E., Kealhofer, D. A., Carn, E. K., Serwane, F., Lucio, A. A., Giammona, J. and Campas, O. (2018). A fluid-to-solid jamming transition underlies vertebrate body axis elongation. *Nature* **561**, 401-405. doi:10.1038/s41586-018-0479-2
Moreno-Mateos, M. A., Vejnar, C. E., Beaudoin, J. D., Fernandez, J. P., Mis, E. K., Khokha, M. K. and Giraldez, A. J. (2015). CRISPRscan: designing highly efficient sgRNAs for CRISPR-Cas9 targeting in vivo. *Nat. Methods* **12**, 982-988. doi:10.1038/nmeth.3543
Morley, R. H., Lachani, K., Keefe, D., Gilchrist, M. J., Flicek, P., Smith, J. C. and Wardle, F. C. (2009). A gene regulatory network directed by zebrafish No tail accounts for its roles in mesoderm formation. *Proc. Natl. Acad. Sci. USA* **106**, 3829-3834. doi:10.1073/pnas.0808382106
Morrow, Z. T., Maxwell, A. M., Hoshijima, K., Talbot, J. C., Grunwald, D. J. and Amacher, S. L. (2017). tbx6l and tbx16 are redundantly required for posterior paraxial mesoderm formation during zebrafish embryogenesis. *Dev. Dyn.* **246**, 759-769. doi:10.1002/dvdy.24547
Nowotschin, S., Ferrer-Vaquer, A., Concepcion, D., Papaioannou, V. E. and Hadjantonakis, A. K. (2012). Interaction of Wnt3a, Msgn1 and Tbx6 in neural versus paraxial mesoderm lineage commitment and paraxial mesoderm differentiation in the mouse embryo. *Dev. Biol.* **367**, 1-14. doi:10.1016/j.ydbio.2012.04.012
Olivera-Martinez, I., Harada, H., Halley, P. A. and Storey, K. G. (2012). Loss of FGF-dependent mesoderm identity and rise of endogenous retinoid signalling determine cessation of body axis elongation. *PLoS Biol.* **10**, e1001415. doi:10.1371/journal.pbio.1001415
Payumo, A. Y., McQuade, L. E., Walker, W. J., Yamazoe, S. and Chen, J. K. (2016). Tbx16 regulates hox gene activation in mesodermal progenitor cells. *Nat. Chem. Biol.* **12**, 694-701. doi:10.1038/nchembio.2124
Pourquié, O. (2018). Somite formation in the chicken embryo. *Int. J. Dev. Biol.* **62**, 57-62. doi:10.1387/ijdb.180036op
Provost, E., Rhee, J. and Leach, S. D. (2007). Viral 2A peptides allow expression of multiple proteins from a single ORF in transgenic zebrafish embryos. *Genesis* **45**, 625-629. doi:10.1002/dvg.20338
Row, R. H. and Kimelman, D. (2009). Bmp inhibition is necessary for post-gastrulation patterning and morphogenesis of the zebrafish tailbud. *Dev. Biol.* **329**, 55-63. doi:10.1016/j.ydbio.2009.02.016
Schmittgen, T. D. and Livak, K. J. (2008). Analyzing real-time PCR data by the comparative C(T) method. *Nat. Protoc.* **3**, 1101-1108. doi:10.1038/nprot.2008.73
Schulte-Merker, S., van Eeden, F. J., Halpern, M. E., Kimmel, C. B. and Nusslein-Volhard, C. (1994). no tail (ntl) is the zebrafish homologue of the mouse T (Brachyury) gene. *Development* **120**, 1009-1015.
Sive, H. L., Draper, B. W., Harland, R. M. and Weintraub, H. (1990). Identification of a retinoic acid-sensitive period during primary axis formation in Xenopus laevis. *Genes Dev.* **4**, 932-942. doi:10.1101/gad.4.6.932
Steventon, B. and Martinez Arias, A. (2017). Evo-engineering and the cellular and molecular origins of the vertebrate spinal cord. *Dev. Biol.* **432**, 3-13. doi:10.1016/j.ydbio.2017.01.021
Suemori, H. and Noguchi, S. (2000). Hox C cluster genes are dispensable for overall body plan of mouse embryonic development. *Dev. Biol.* **220**, 333-342. doi:10.1006/dbio.2000.9651
Talbot, J. C. and Amacher, S. L. (2014). A streamlined CRISPR pipeline to reliably generate zebrafish frameshifting alleles. *Zebrafish* **11**, 583-585. doi:10.1089/zeb.2014.1047
Tsakiridis, A., Huang, Y., Blin, G., Skylaki, S., Wymeersch, F., Osorno, R., Economou, C., Karagianni, E., Zhao, S., Lowell, S. et al. (2014). Distinct Wnt-driven primitive streak-like populations reflect in vivo lineage precursors. *Development* **141**, 1209-1221. doi:10.1242/dev.101014
Turner, D. A., Hayward, P. C., Baillie-Johnson, P., Rue, P., Broome, R., Faunes, F. and Martinez Arias, A. (2014). Wnt/beta-catenin and FGF signalling direct the specification and maintenance of a neuromesodermal axial progenitor in ensembles of mouse embryonic stem cells. *Development* **141**, 4243-4253. doi:10.1242/dev.112979
Wilson, V., Olivera-Martinez, I. and Storey, K. G. (2009). Stem cells, signals and vertebrate body axis extension. *Development* **136**, 1591-1604. doi:10.1242/dev.021246
Wittler, L., Shin, E. H., Grote, P., Kispert, A., Beckers, A., Gossler, A., Werber, M. and Herrmann, B. G. (2007). Expression of Msgn1 in the presomitic mesoderm is controlled by synergism of WNT signalling and Tbx6. *EMBO Rep.* **8**, 784-789. doi:10.1038/sj.embor.7401030
Wymeersch, F. J., Huang, Y., Blin, G., Cambray, N., Wilkie, R., Wong, F. C. K. and Wilson, V. (2016). Position-dependent plasticity of distinct progenitor types in the primitive streak. *Elife* **5**, e10042. doi:10.7554/eLife.10042
Wymeersch, F. J., Skylaki, S., Huang, Y., Watson, J. A., Economou, C., Marek-Johnston, C., Tomlinson, S. R. and Wilson, V. (2019). Transcriptionally dynamic progenitor populations organised around a stable niche drive axial patterning. *Development* **146**, dev168161. doi:10.1242/dev.168161
Yabe, T. and Takada, S. (2012). Mesogenin causes embryonic mesoderm progenitors to differentiate during development of zebrafish tail somites. *Dev. Biol.* **370**, 213-222. doi:10.1016/j.ydbio.2012.07.029
Yamamoto, A., Amacher, S. L., Kim, S. H., Geissert, D., Kimmel, C. B. and De Robertis, E. M. (1998). Zebrafish paraxial protocadherin is a downstream target of spadetail involved in morphogenesis of gastrula mesoderm. *Development* **125**, 3389-3397.
Yoo, K.-W., Kim, C.-H., Park, H.-C., Kim, S.-H., Kim, H.-S., Hong, S.-K., Han, S., Rhee, M. and Huh, T.-L. (2003). Characterization and expression of a presomitic mesoderm-specific mespo gene in zebrafish. *Dev. Genes Evol.* **213**, 203-206. doi:10.1007/s00427-003-0312-1
Young, T., Rowland, J. E., van de Ven, C., Bialecka, M., Novoa, A., Carapuco, M., van Nes, J., de Graaff, W., Duluc, I., Freund, J. N. et al. (2009). Cdx and Hox genes differentially regulate posterior axial growth in mammalian embryos. *Dev. Cell* **17**, 516-526. doi:10.1016/j.devcel.2009.08.010
Zheng, C. and Chalfie, M. (2016). Securing neuronal cell fate in C. elegans. *Curr. Top. Dev. Biol.* **116**, 167-180. doi:10.1016/bs.ctdb.2015.11.011
Zheng, C., Jin, F. Q. and Chalfie, M. (2015). Hox proteins act as transcriptional guarantors to ensure terminal differentiation. *Cell Rep.* **13**, 1343-1352. doi:10.1016/j.celrep.2015.10.044

SUPPLEMENTARY FIGURES

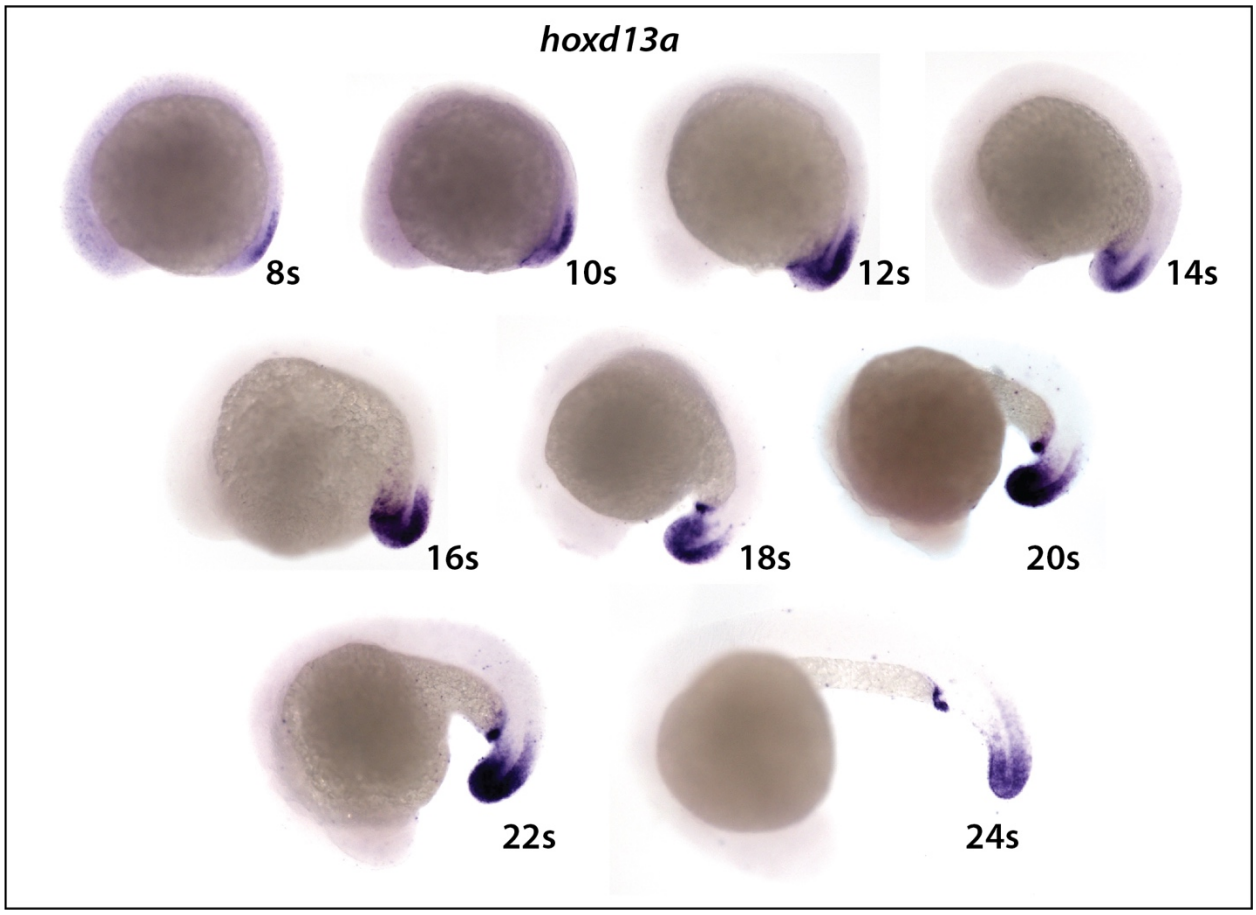

Figure S1 *hoxd13a* is expressed from early stages of embryogenesis. Refers to Figure 1.

Expression of *hoxd13a* from 8s until the 24s. Embryos from 12s to 24s were developed for the same length of time. Embryos at 8s and 10s were developed twice as long.

Figure S2 Adult *hoxa13b;d13a* mutant. Refers to Figure 2.

Shown is a *ntl*$^{cs/cs}$;*hoxa13b*$^{\Delta 16/\Delta 16}$;*d13b*$^{ins4/-}$ mutant that survived to adulthood with severe posterior defects. Most fish with this degree of posterior defect die as larvae.

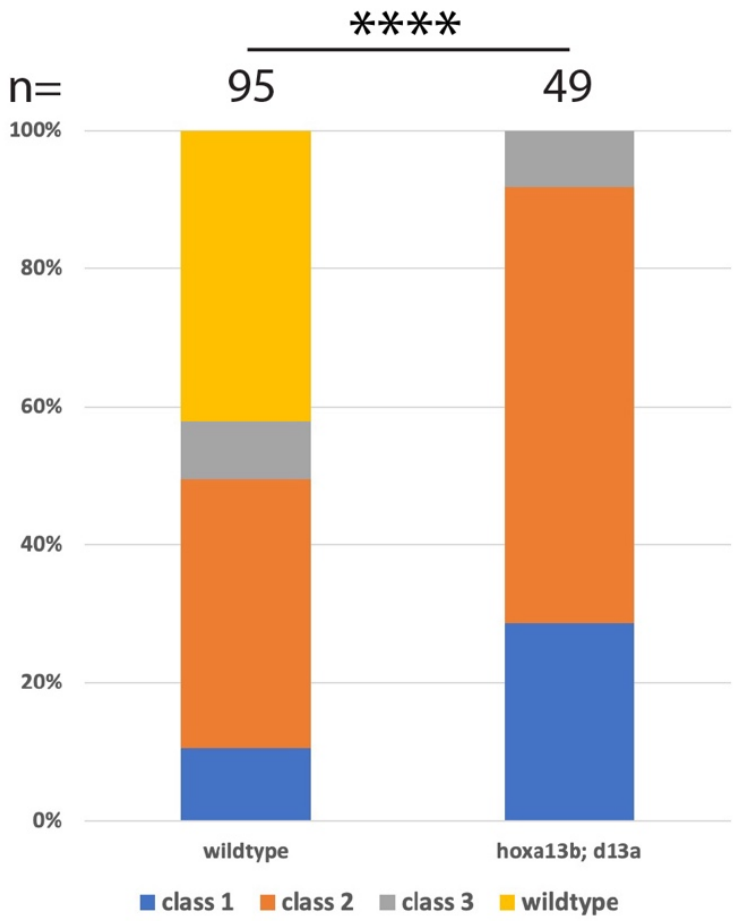

Figure S3 *Hoxa13b;d13a* mutants in a *ntl* wildtype background are hypersensitive to Tbxta reduction. Refers to Figure 3.

Embryos from a cross of wildtype or *hoxa13;d13* mutant fish (in a $ntl^{+/+}$ background) were injected with very low doses (0.2 ng) of a *tbxta* morpholino. The *hoxa13;d13* mutant fish show enhanced defects relative to wildtype fish. **** = p<0.0001, Fisher's Exact test.

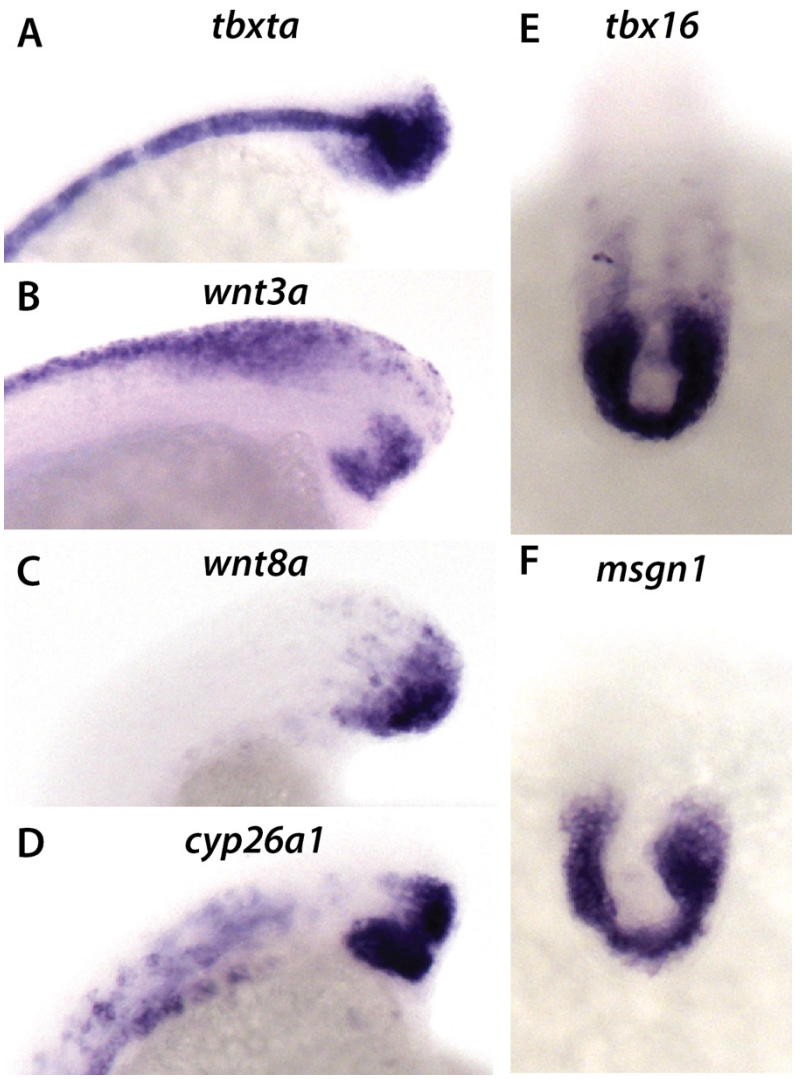

Figure S4 Reduction of mesodermal gene expression in *ntl*^{cs} embryos at 18.5° C. Refers to Figure 4.

A-F) In situ hybridization of class 1 15s *ntl*^{cs} homozygous embryos maintained at 18.5° C. Compare to the wildtype expression patterns shown in Figure 4. The reduction of mesodermal genes is the same as observed in in *hoxa13;ntl*^{cs} embryos maintained at 18.5°C.

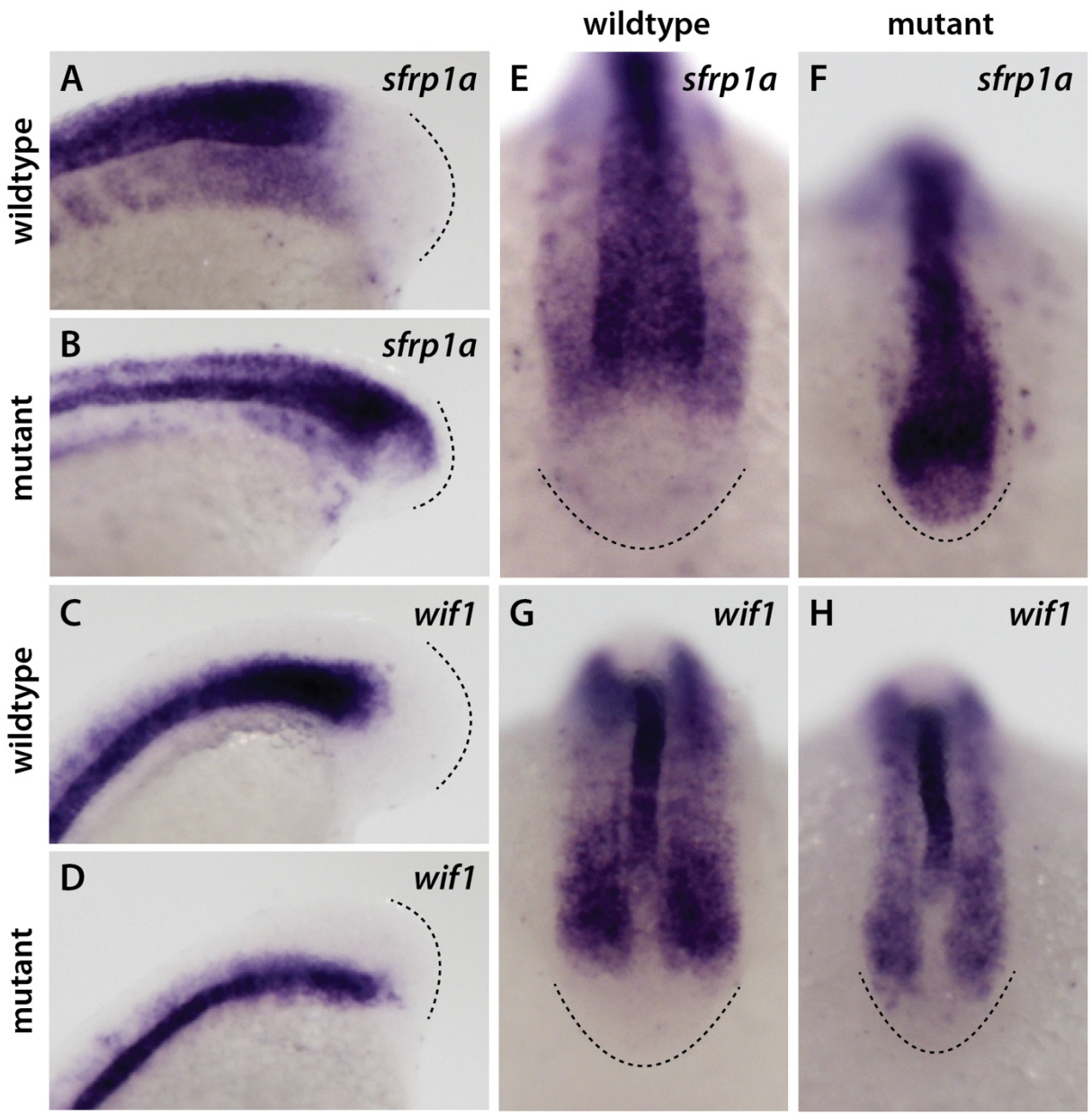

Figure S5 Wnt inhibitors expressed more posteriorly in *hoxa13;ntl*^{cs} embryos at 18.5° C. Refers to Figure 4.

(A-H) In situ hybridization of wildtype and *hoxa13;ntl*^{cs} embryos at 15s. Note that both genes expand more posteriorly in the mutants. Mutants with expanded expression: *sfrp1a* (81%, n=26) and *wif1* (79%, n=24). A-D are lateral views and panels E-H are dorsal views. The posterior limit of the tailbud is shown by a line.

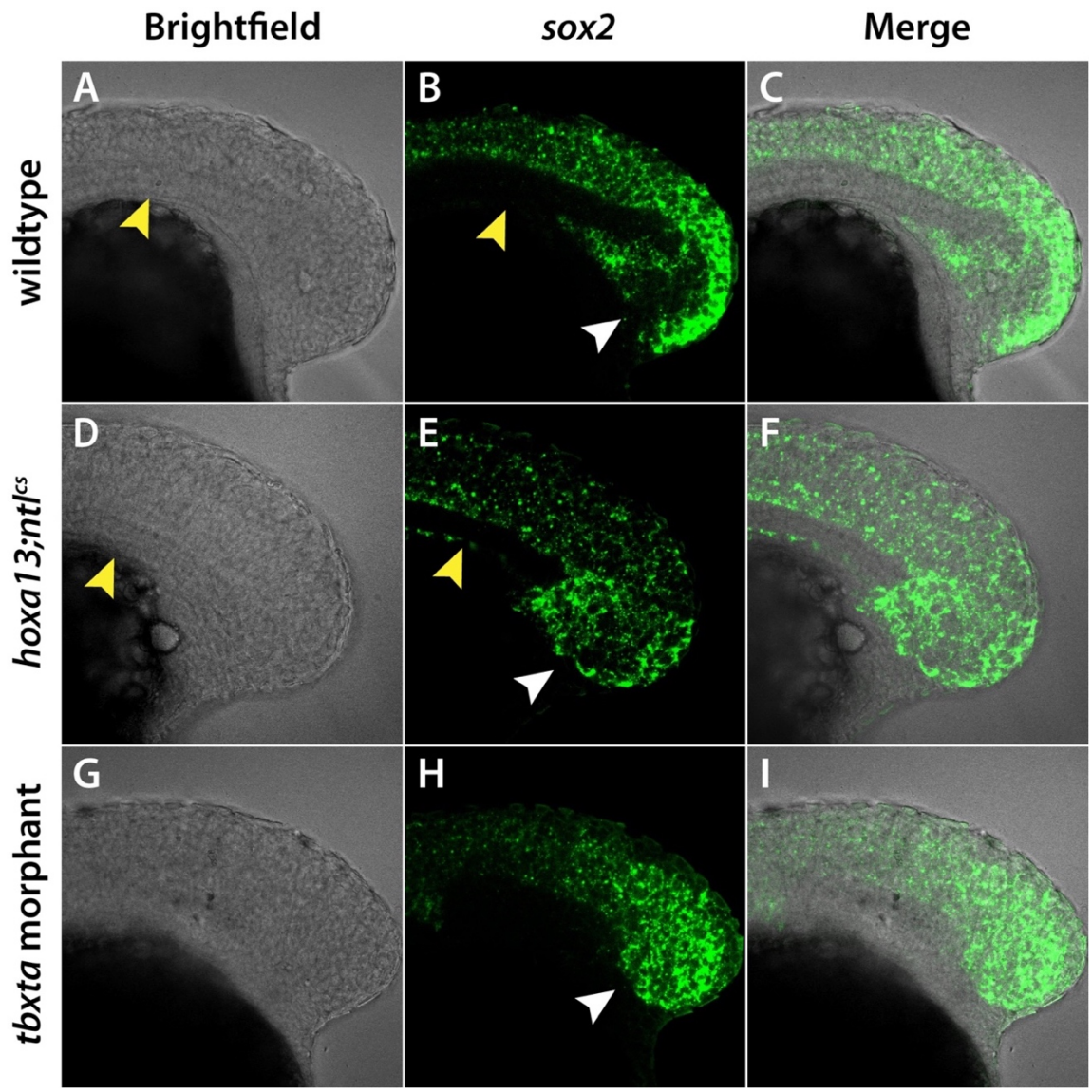

Figure S6 *sox2* expression expands into the mesodermal progenitor region in *hoxa13;ntl*^{cs} mutants at 18.5° C.

A-C) In wildtype embryos *sox2* is present in the NMps and neural tube, but absent from the mesodermal progenitor zone (white arrowhead). D-F) In *hoxa13;ntl*^{cs} mutants *sox2* expands into the mesodermal progenitor zone (white arrowhead). F-I) in *tbxta/ntl* morphants *sox2* also expands into the mesodermal progenitor zone, as was previously shown for *tbxta/ntl* mutants (Martin and Kimelman, 2012). In both brightfield and fluorescent imaging the notochord is visible in wildtype and *hoxa13;ntl*^{cs} mutants (yellow arrowheads in panels A,B,D and E) but is not observed in *tbxta/ntl* morphants. Embryos are at the 15s stage and are shown in a side view of a confocal section at the midline of the embryo.

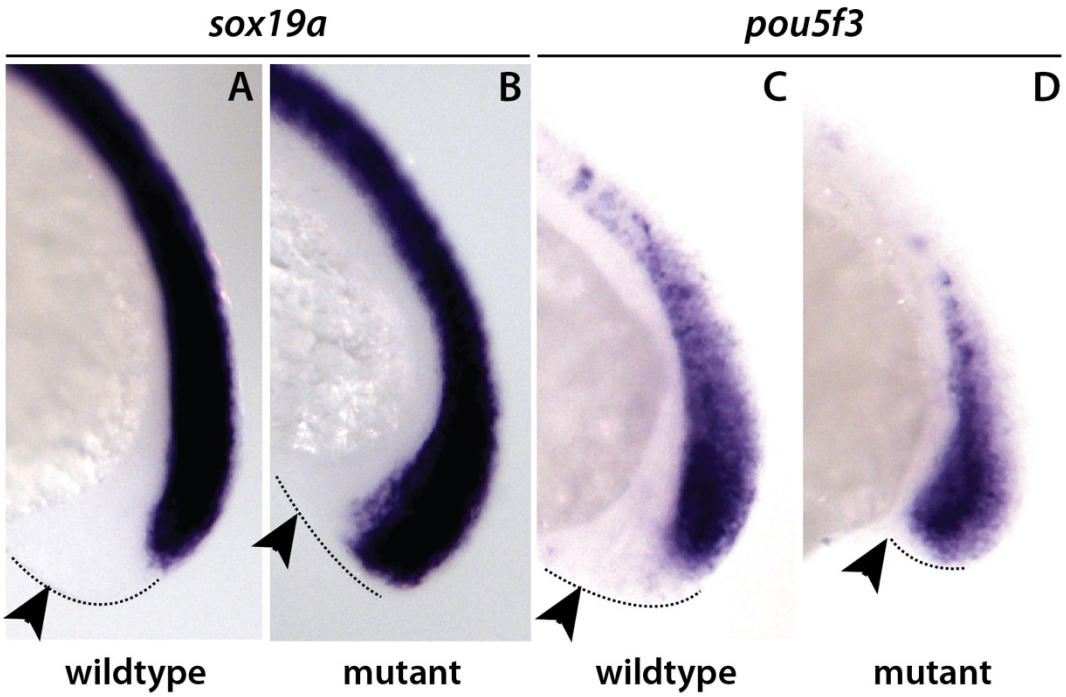

Figure S7 *sox19a and pou5f3* expression expands into the mesodermal progenitor region in *hoxa13;ntl^{cs}* mutants at 18.5° C. Refers to Figure 4.

A-D) In situ hybridization of 15s wildtype and *hoxa13;ntl^{cs}* embryos for the neural markers *sox19a* and *pou5f3*. As with *sox2*, expression expands into the prospective mesodermal territory in the *hoxa13;ntl^{cs}* mutants.

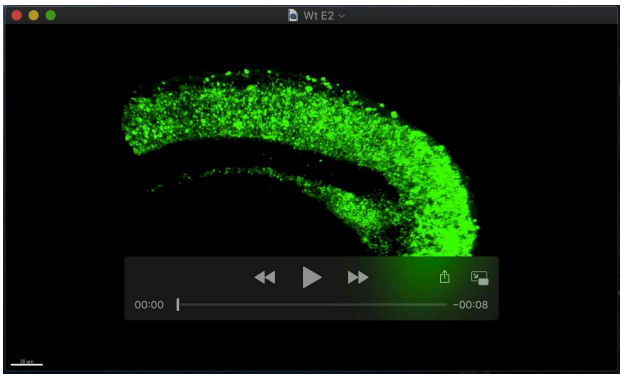

Movie 1. *sox2* expression in a wildtype embryo.
The same embryo as in Figure S6A-C.

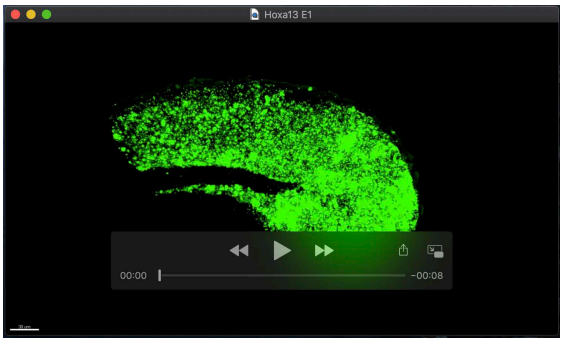

Movie 2. *sox2* expression in a *hoxa13;ntl*^{cs} mutant with a class 1 phenotype.
The same embryo as in Figure S6D-F.

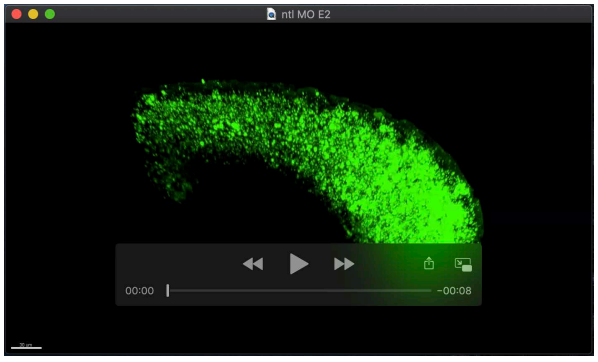

Movie 3. *sox2* expression in a *tbxta/ntl* morphant.
The same embryo as in Figure S6G-I.